

LAMOST Views δ Scuti Pulsating Stars

Qian S.-B.^{1,2,3,4}, Li L.-J.^{1,2,3}, He J.-J.^{1,2,3}, Zhang J.^{1,2,3}, Zhu L.-Y.^{1,2,3,4}, Shi X.-D.^{1,2,3,4},
Zhao E.-G.^{1,2,3,4}, and Han Z.-T.^{1,2,3,4}

ABSTRACT

700 δ Scuti pulsating stars were observed by LAMOST by November 30, 2016. Stellar atmospheric parameters of 463 variables were determined, while spectral types were obtained for all samples. In the paper, those spectroscopic data are catalogued. We present a group of 113 unusual and cool variable stars (UCVs) that are distinguished from the normal δ Scuti stars (NDSTs). On the H-R diagram and the $\log g - T$ diagram, the UCVs are far beyond the red edge of pulsational instability trip. Their effective temperatures are lower than 6700 K with periods in the range from 0.09 to 0.22 days. NDSTs have metallicity close to that of the Sun as expected, while UCVs are more metal poor than NDSTs. It is shown that those UCVs may not belong to δ Scuti stars because their pulsation constants (Q) are usually higher than 0.033 days. The two peaks on the distributions of the period, the temperature, the gravitational acceleration, and the metallicity are all caused by the existence of UCVs. When those UCVs are excluded, it is discovered that the effective temperature, the gravitational acceleration and the metallicity all are correlated with the pulsating period for NDSTs and their physical properties and evolutionary states are discussed. The detecting of those UCVs indicates that about 24% of the known δ Scuti stars were misclassified and some in the period range from 0.09 to 0.22 days should be reclassified. If some of them are confirmed to be pulsating stars, they will be a new-type pulsators and their investigations will shed light on theoretical instability domains and on the theories of interacting between the pulsation and

¹Yunnan Observatories, Chinese Academy of Sciences (CAS), P.O. Box 110, 650011 Kunming, P. R. China (e-mail: qsb@ynao.ac.cn)

²Key laboratory of the structure and evolution of celestial objects, Chinese Academy of Sciences, P.O. Box 110, 650011 Kunming, P. R. China

³Center for Astronomical Mega-Science, Chinese Academy of Sciences, 20A Datun Road, Chaoyang District, Beijing, 100012, P. R. China

⁴University of the Chinese Academy of Sciences, Yuquan Road 19#, Sijingshang Block, 100049 Beijing, P. R. China

the convection of solar-type stars. Meanwhile, 64 δ Scuti stars are detected to be the candidates of binary or multiple systems.

Subject headings: Stars: fundamental parameters – Stars: oscillations — Stars: binaries : spectroscopic – Stars: variables: other

1. Introduction

The δ Scuti-type pulsating stars lie inside the classical cepheid instability strip with luminosity classes range between III and V (e.g., Breger 1979, 2000; Lopez de Coca et al. 1990; Rodríguez et al. 2000). Their spectral types are range between A2 and F5 and have masses between 1.4 and $3 M_{\odot}$. δ Scuti stars exhibit both radial and non-radial pulsations with frequencies ranging between 3 and 80 d^{-1} and can oscillate in both p and g modes. These properties make them a good target for astroseismology investigations and thus study stellar interiors and stellar evolution. The pulsating amplitudes of classical δ Scuti stars are usually in the range of 0.003-0.9 mag in the V band, with periods usually between 0.02 and 0.3 days (e.g., Breger 1979; Chang et al. 2013). Their great number of radial and non-radial pulsation modes are mainly driven by the κ mechanism that are mostly working in the He II ionization zone (e.g., Gautschy & Saio 1995; Breger et al. 2005; Rodríguez & Breger 2001). The theoretical blue edge of δ Scuti instability trip was well determined (e.g., Pamyatnykh 2000), while the red edge is rather complicated because of the coupling between convection and oscillation together with the turbulent viscosity (e.g., Xiong & Deng 2001). In the recent catalogue of δ Scuti pulsating stars, about 18 ones including VX Hya (F6) and DE Lac (F7) were reported to be beyond the red edge and thus have cool temperatures with the spectroscopic/photometric spectral types later then F5 (e.g., Chang et al. 2013).

A large number of δ Scuti stars were discovered by several photometric surveys in the world, e.g., All Sky Automated Survey (ASAS, Pojmanski 1997; Pojmanski et al. 2005), the asteroid survey LINEAR (Palaversa et al. 2013), and Northern sky variability survey (NSVS, Woźniak et al. 2004). In particular, the Kepler (Borucki et al. 2010) space telescopes have produced high-quality data sets for thousands of stars and about 2000 δ Scuti stars were detected (e.g., Balona & Dziembowski 2011; Uytterhoeven et al. 2011). Since the data on variable stars including δ Scuti stars are constantly varying, the mission of VSX (the international variable star index) is bringing all of new information together in a single data repository (e.g., Watson 2006). To date, about 3688 δ Scuti variable stars have been detected and were listed in VSX by March 13, 2017. Those photometric survey data are very useful to understand the photometric properties of δ Scuti variable stars. However, their spectroscopic information including spectral types and stellar atmospheric parameters

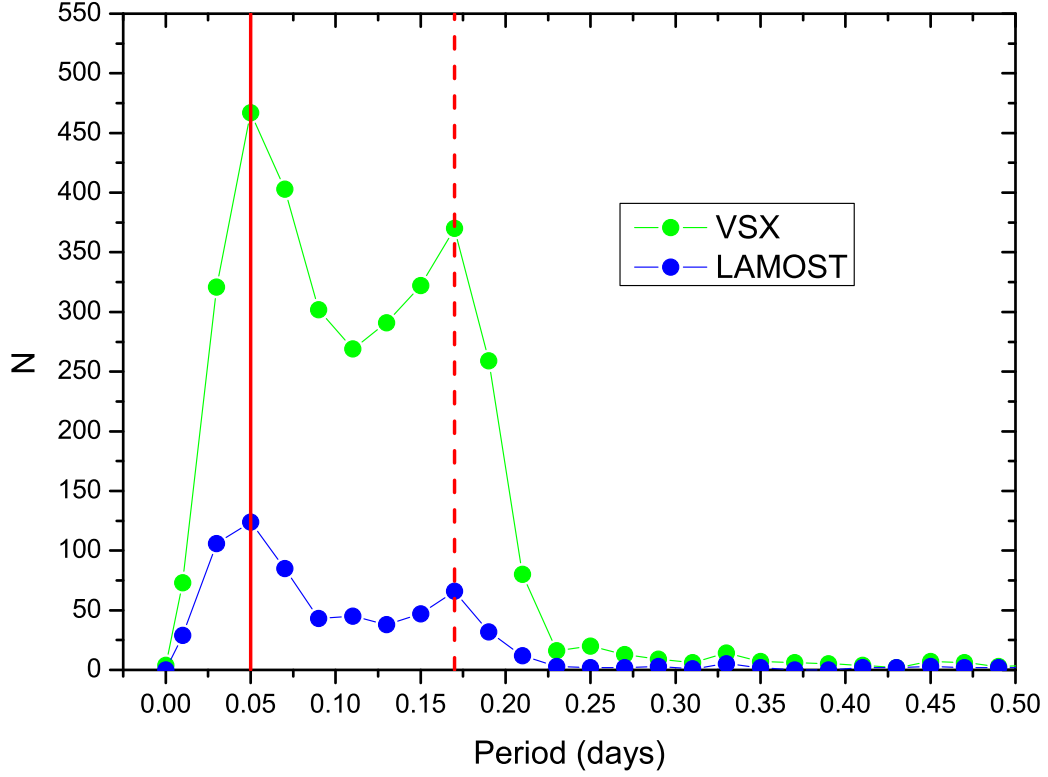


Fig. 1.— Period distributions of δ Scuti pulsating stars. Blue and Green dots represent δ Scuti variables observed by LAMOST and listed in VSX catalogue, respectively. Solid red line refers to the main peak near 0.05 days, while the dashed red line to the other small peak near 0.17 days.

is extremely lack. Among 1578 δ Scuti stars collected by Chang et al. (2013), only 15% of them have spectroscopic spectral types.

LAMOST (Large Sky Area Multiobject Fiber Spectroscopic Telescope, also called as Guo Shou Jing telescope) is a special telescope that has a field of view of 5 degree and could simultaneously obtain the spectra of about 4000 stars with low-resolution of about 1800 in a one exposure (Wang et al. 1996; Cui et al. 2012). The wavelength range of LAMOST is from 3700 to 9000 Å and is divided in two arms, i.e., a blue arm (3700-5900 Å) and a red arm (5700-9000 Å). Huge amounts of spectroscopic data have been obtained for single stars and close binaries (e.g., Zhao et al. 2012, Luo et al. 2015; Qian et al. 2017). In the time interval between October 24, 2011 and November 30, 2016, 700 δ Scuti pulsating stars were observed by LAMOST. In the recent LAMOST data releases, stellar atmospheric parameters for 463 δ Scuti stars were determined when their spectra have higher signal to noise, while spectral types of all variables were obtained. Those spectroscopic data provide valuable information on their physical properties, evolutionary states and binarities.

Among the 700 observed δ Scuti stars, the pulsating periods of 683 samples are given in VSX. The period distribution for those observed δ Scuti variables is shown in Fig. 1. Also displayed in the figure is the period distribution of 3688 δ Scuti variable stars in VSX where 341 δ Scuti stars without pulsating periods are not shown. The period distribution given by Rodriguez & Breger (2001) indicated that the majority of δ Scuti stars have short periods in the range from 0.05 to 0.1 days and the number is decreasing with increasing period. However, as shown in Fig. 1, there are two peaks in the period distributions. The main peak is near 0.05 days, while the other small peak is at 0.17 days. These properties are similar to those observed in RR Lyr-type pulsating stars (e.g., Szczygiel & Fabrycky 2007). The latter was caused by the known two types of RR Lyr-type pulsating stars, i.e., R Rab and R Rc. In the paper, we report the existence of a group of unusual and cool variable stars (hereafter UCVs) that are distinguished from normal ones. Then the physical properties of normal δ Scuti stars (hereafter NDSTs) are investigated after UCVs are excluded. Finally, based on the distributions of those atmospheric parameters and some statistical correlations, the physical properties, the binarities and the evolutionary states of δ Scuti stars are discussed.

2. Catalogues of spectroscopic observations for UCVs and NDSTs

In the recent LAMOST data releases, about 19.0% δ Scuti-type variables (700) listed in VSX were observed by LAMOST spectroscopic survey from October 24, 2011 to November 30, 2016. Among the 700 δ Scuti stars, stellar atmospheric parameters of 463 δ Scuti stars were determined by using good and reliable spectra. The atmospheric parameters including

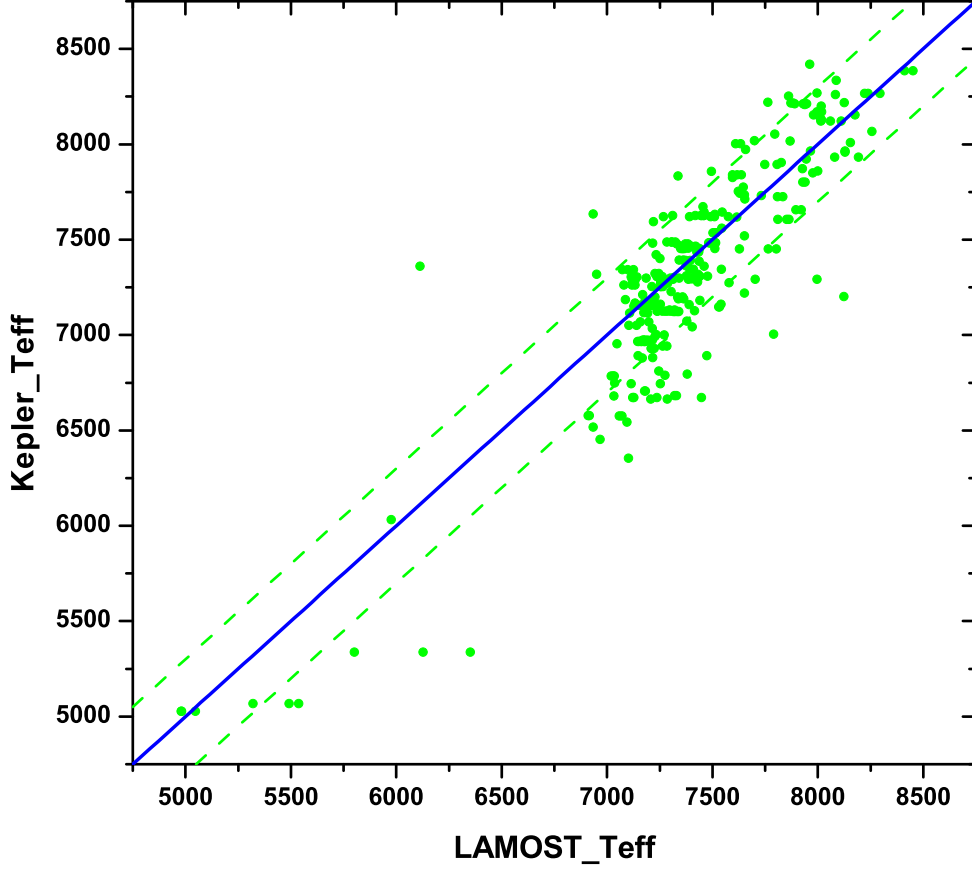


Fig. 2.— Comparison of effective temperatures for those 352 δ Scuti stars that were observed by both LAMOST and Kepler satellite. Their effective temperatures are given in the *Kepler* Input Catalog and obtained by using LAMOST. It is shown that both temperatures for most δ Scuti variables are consistent within 300 K (dashed lines).

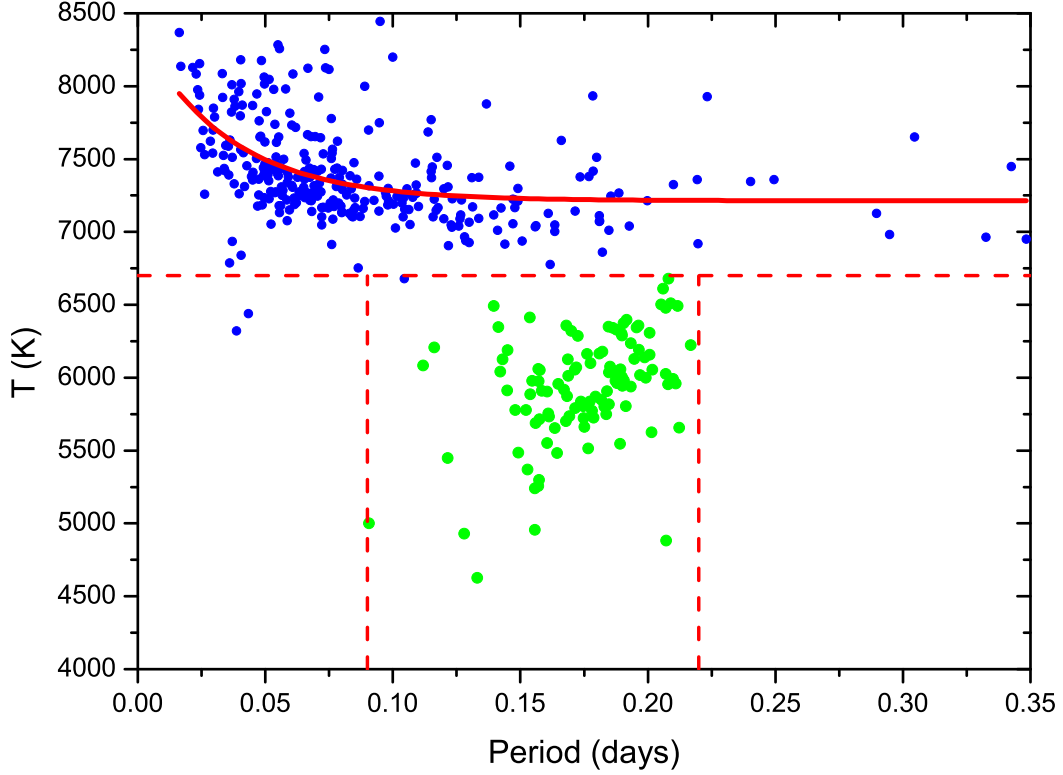


Fig. 3.— Correlation between the pulsating period and the effective temperature for δ Scuti variable stars with periods shorter than 0.35 days. A group of 113 UCVs (green dots) are shown to be distinguished from the normal ones (blue dots). The dashed red lines represent their borders. The UCVs have temperatures lower than 6700 K with pulsating periods in the range from 0.09 to 0.22 days. The solid red line indicates that there is a good relation between the period and the effective temperature for normal δ Scuti stars with period shorter than 0.35 days.

Table 1: Mean stellar atmospheric parameters for 24 δ Scuti stars observed 4 times or more and their standard errors.

| Star Name | Period (days) | Times | \overline{T} (K) | Errors | $\overline{\log g}$ | Errors | $[\text{Fe}/\text{H}]$ | Errors |
|---------------------|---------------|-------|--------------------|--------|---------------------|--------|------------------------|--------|
| KIC 7697795 | 0.057185 | 10 | 7498.35 | 12.26 | 3.854 | 0.007 | 0.078 | 0.007 |
| KIC 10014548 | 0.65445 | 9 | 7210.29 | 16.89 | 3.815 | 0.030 | 0.561 | 0.015 |
| KIC 7106205 | 0.074655 | 7 | 7165.09 | 14.01 | 3.838 | 0.024 | 0.117 | 0.014 |
| KIC 11395392 | 0.039701 | 7 | 7261.43 | 44.62 | 4.128 | 0.024 | -0.251 | 0.017 |
| ASAS J075941-0353.1 | 0.180982 | 6 | 7072.65 | 33.10 | 3.752 | 0.027 | 0.173 | 0.02 |
| KIC 3942911 | 0.03391 | 6 | 7436.53 | 20.79 | 3.956 | 0.017 | 0.047 | 0.015 |
| KID 07900367 | 0.075489 | 5 | 7197.27 | 13.10 | 3.805 | 0.012 | 0.513 | 0.007 |
| KIC 11127190 | 0.053387 | 5 | 7446.18 | 16.22 | 3.920 | 0.012 | 0.253 | 0.007 |
| BS Cnc | 0.051 | 4 | 7476.40 | 17.27 | 3.902 | 0.023 | 0.062 | 0.017 |
| BW Cnc | 0.072 | 4 | 7430.03 | 41.70 | 3.903 | 0.016 | 0.129 | 0.013 |
| ASAS J064626+2629.8 | 0.205972 | 4 | 6609.64 | 10.17 | 4.163 | 0.025 | -0.249 | 0.007 |
| ASAS J071540+2022.2 | 0.200724 | 4 | 6306.72 | 4.34 | 4.168 | 0.013 | -0.079 | 0.013 |
| V0367 Cam | 0.121596 | 4 | 7307.84 | 122.89 | 3.857 | 0.023 | 0.188 | 0.049 |
| ASAS J190751+4629.2 | 0.079561 | 4 | 7178.47 | 7.23 | 3.912 | 0.035 | 0.185 | 0.016 |
| KIC 10002897 | 0.064965 | 4 | 7305.43 | 16.86 | 4.062 | 0.014 | -0.104 | 0.052 |
| BD+24 95 | 0.11992 | 4 | 7089.90 | 19.54 | 3.750 | 0.005 | 0.490 | 0.024 |
| KIC 8869892 | 0.12989 | 4 | 7067.90 | 23.43 | 3.884 | 0.089 | -0.098 | 0.134 |
| KIC 9324334 | 0.097352 | 4 | 7246.62 | 23.53 | 3.968 | 0.030 | 0.124 | 0.022 |
| KIC 10615125 | 0.10351 | 4 | 7198.83 | 13.85 | 3.821 | 0.008 | 0.340 | 0.011 |
| KIC 4488840 | 0.063279 | 4 | 7274.49 | 26.09 | 3.925 | 0.011 | 0.058 | 0.016 |
| KIC 8149341 | 0.037015 | 4 | 7511.14 | 5.75 | 3.854 | 0.012 | 0.167 | 0.007 |
| KIC 9391395 | 0.51308 | 4 | 7246.77 | 11.46 | 4.046 | 0.010 | -0.198 | 0.008 |
| KIC 9775385 | 0.55928 | 4 | 7358.38 | 7.40 | 3.984 | 0.011 | 0.072 | 0.005 |
| GSC 01946-00035 | 0.067081 | 4 | 7264.50 | 44.51 | 3.997 | 0.015 | -0.028 | 0.031 |

the effective temperature T , the gravitational acceleration $\log g$, the metallicity $[\text{Fe}/\text{H}]$ and the radial velocity V_r were automatically determined by the LAMOST stellar parameter pipeline that is based on the Universite de Lyon spectroscopic analysis software (ULySS) (e.g., Koleva et al. 2009; Wu et al. 2011, 2014; Luo et al. 2015). The ULySS fits the full observed spectra by using the model spectrum that is generated by an interpolator by using the ELODIE library as a reference (e.g., Prugniel & Soubiran 2001). The standard deviations are 110 K, 0.19 dex and 0.11 dex for T , $\log g$ and $[\text{Fe}/\text{H}]$ respectively when $T < 8000$ K. As for the radial velocity V_r , when $T < 10000$ K the standard deviations are 4.91 km s^{-1} (e.g., Gao et al. 2015).

The temperatures of all targets are below 8500 K, their atmospheric parameters could be determined well. There are 24 δ Scuti variable stars were observed four times or more on different dates. To check the reliability of stellar atmospheric parameters, we determined the mean values of their atmospheric parameters and derived the corresponding standard errors. The results are shown in Table 1 where their names and pulsating periods are listed in the first and the second columns. The observational times are shown in third column, while the average atmospheric parameters and their standard errors are displayed in the

rest columns. As shown in Table 1, apart from one target, the standard errors of the effective temperature for the rest targets are lower than 50 K, while the standard errors of the gravitational acceleration $\log g$ are lower than 0.09 dex. As for the metallicity, apart from one target, the standard errors for most δ Scuti variable stars targets are lower than 0.06 dex. These results may indicate that errors of δ Scuti stars are within those for normal stars. About 2000 δ Scuti variables were found by the Kepler space telescopes (e.g., Balona & Dziembowski 2011; Uytterhoeven et al. 2011). 352 of them were also observed by LAMOST from October 24, 2011 to November 30, 2016 and their effective temperatures have been given in the *Kepler* Input Catalog (KIC)¹. The comparison of effective temperatures given in KIC and obtained by using LAMOST is shown in Fig. 2. As displayed in the figure, most of the effective temperatures are in agreement with each other within 300 K.

The correlation between the pulsating period P and the effective temperature T for those observed δ Scuti stars is displayed in Fig. 3. The pulsating periods in the figure are from VSX² (e.g., Watson, 2006). As shown in Fig. 3, there is a group of 113 UCVs (green dots) that are clearly separated from the other 350 variable stars (blue dots) indicating that they are a group of unusual variable stars. The dashed red lines in the figure represent the borders of UCVs. Their temperatures are lower than 6700 K and the periods are in the range from 0.09 to 0.22 days. The observations of the 113 UCVs are catalogued in the order of increasing VSX number. Some of them were observed twice or more times on different dates and we list all of the parameters (149 sets of data in total). Those listed in Table 2 are the first 50 observations. The whole catalogue is available in the internet electronic version and it will be improved by adding new data obtained by LAMOST in the future. Table 2 includes star names, their right ascensions (RA) and declinations (DEC), types of light variation and pulsating periods. These parameters are from VSX catalogue. Column 6 lists the distances (in arcsec) between the two positions determined by the coordinates given in VSX and by LAMOST. As pointed by Qian et al. (2017), the distances were used to identify those δ Scuti variable stars from the LAMOST samples based on the criterion $\text{Dist} < 2$ arcsecs. The observing dates are shown in column 7, while the determined spectral types are listed in columns 8. The stellar atmospheric parameters including T , $\log g$, $[\text{Fe}/\text{H}]$ and V_r , are listed in columns 9, 11, 13 and 15. Their corresponding errors E_1 , E_2 , E_3 and E_4 are also displayed in the table, respectively.

The stellar atmospheric parameters of the other 350 NDSTs are also catalogued. The first 50 observations are shown in Table 3 in the order of increasing VSX number. The

¹<http://archive.stsci.edu/kepler/>

²<http://www.aavso.org/vsx/>

arrangement of the table is the same as those in Table 2. The types of light variation are defined in the GCVS variability classification scheme ³ (e.g., Samus et al. 2017). Some NDSTs were observed twice or more times on different dates and we list all of the stellar parameters. In total, 549 sets of spectroscopic observations were catalogued for the 350 NDSTs. For some δ Scuti stars, their spectra signals to noise are not high enough to determine the stellar atmospheric parameters and thus only spectral types were given. The spectral types of those δ Scuti variable stars are catalogued and those shown in Table 4 are the first 50 spectral types in the catalogue. The catalogue lists 477 spectral types for 304 δ Scuti variable stars. The descriptions of those columns are the same as those in Tables 2 and 3. For about 182 δ Scuti stars, only spectral type was obtained by LAMOST. Both spectral types and stellar atmospheric parameters were determined for 463 δ Scuti stars. For the rest ones, no results were obtained. As done for the previous two catalogues, this whole catalogue is also available in the internet electronic version.

3. Distributions of stellar atmospheric parameters and Binarity for δ Scuti variables

As aforementioned, the stellar atmospheric parameters of 463 δ Scuti pulsating stars were determined. In this section, we investigate the properties of the δ Scuti stars by using those spectroscopic data. During the analyses, when the δ Scuti variables were observed two times or more by LAMOST, the effective temperature T , the gravitational acceleration $\log g$ and the metallicity $[\text{Fe}/\text{H}]$ are averaged and we use the mean values. As for the radial velocity V_r , we do not average them and use the individual values. The distribution of the effective temperature for 463 δ Scuti stars observed by LAMOST is shown in Fig. 4 as blue dots. As displayed in the figure, there are two peaks in the distribution. The main peak is at 7150 K, while the other small peak is near 5950 K. Also shown in the figure as green dots is the temperature distribution for the 113 UCVs. It suggests that the small peak is caused by the existence of the UCVs indicating that they are solar-type cool stars.

The distribution of the gravitational acceleration $\log g$ is plotted in Fig. 5. The main peak of the distribution is near 3.85. Apart from the main peak, there is a small peak at 4.06. These properties reveal that δ Scuti variable stars populate on the instability strip slightly above the zero-age main sequence (ZAMS), the main sequence, and the early stages of H-shell burning. The green dots in the figure represent the distribution of the gravitational acceleration $\log g$ for UCVs where the peak is at 4.13 indicating that their gravitational

³<http://www.sai.msu.su//gcvsv/gcvsv/iii/vartype.txt>

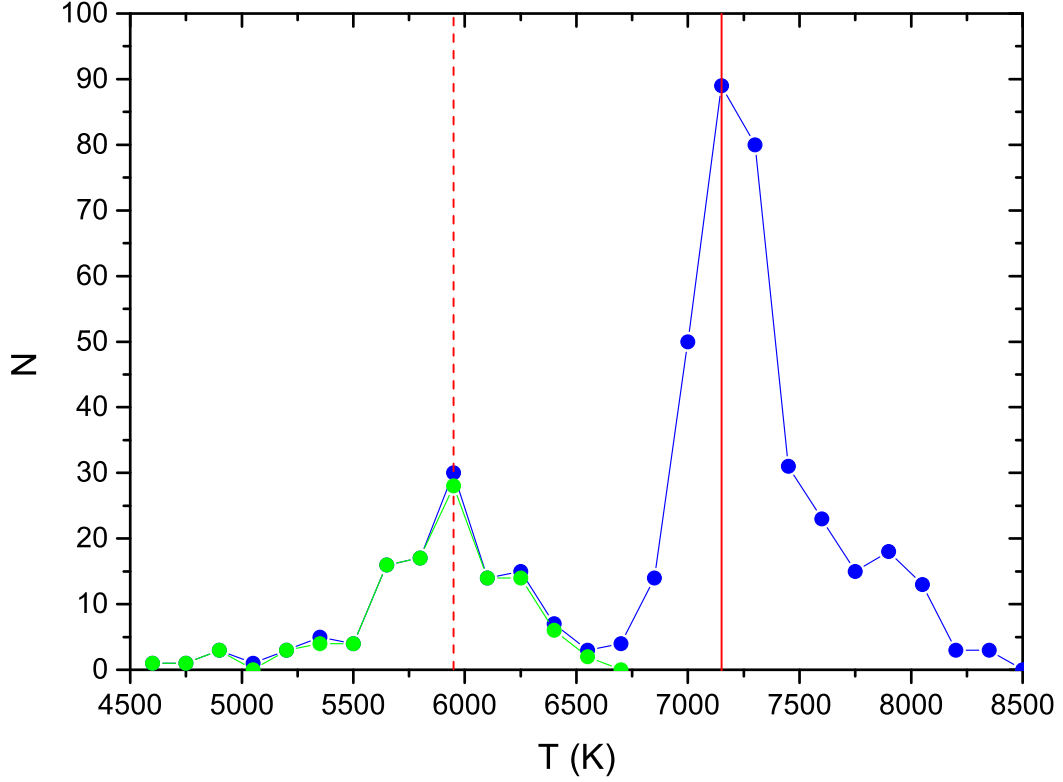


Fig. 4.— Distribution of the effective temperature for whole δ Scuti variable stars whose stellar atmospheric parameters were determined by LAMOST (blue dots). The solid red line refers to the main peak near 7150 K, while the dashed red line to the small peak near 5950 K. The temperature distribution for the 113 UCVs (green dots) is also plotted. It is shown that the small peak is constructed by the existence of the group of cool variable stars.

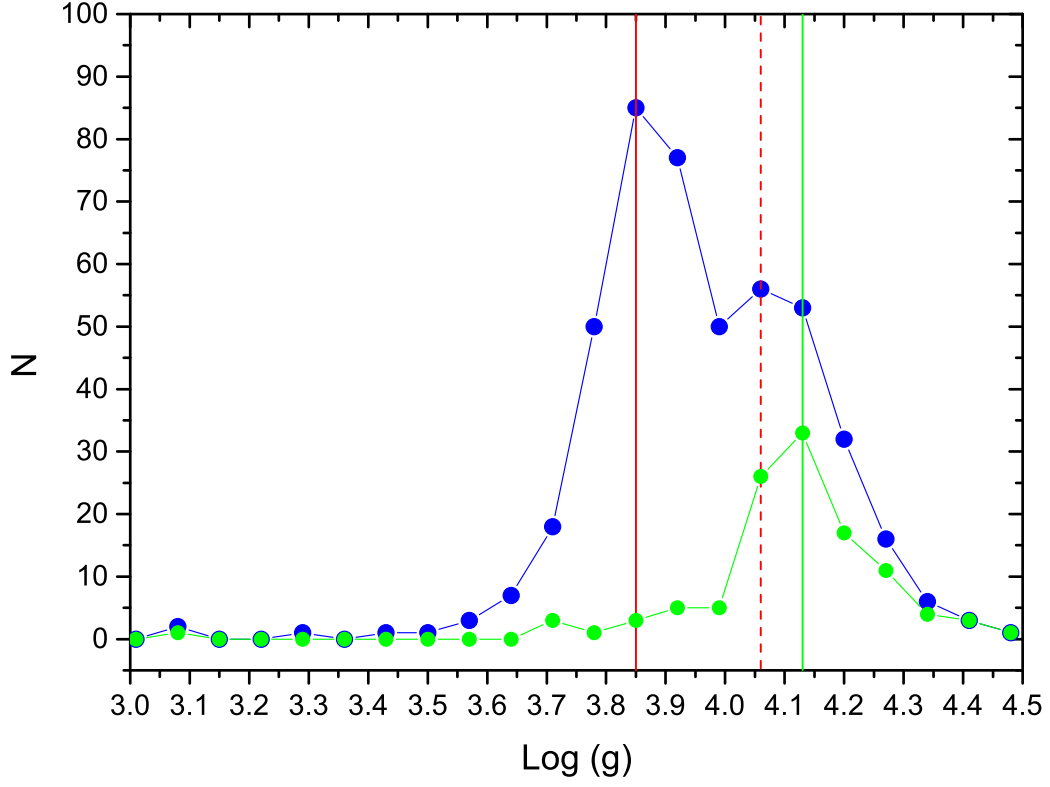


Fig. 5.— Distribution of the gravitational acceleration $\log g$. The solid and the dashed lines represent to the two peaks near 3.85 and 4.06, respectively. The green line refers to the peak for UCVs. Symbols are the same as those in Fig. 4.

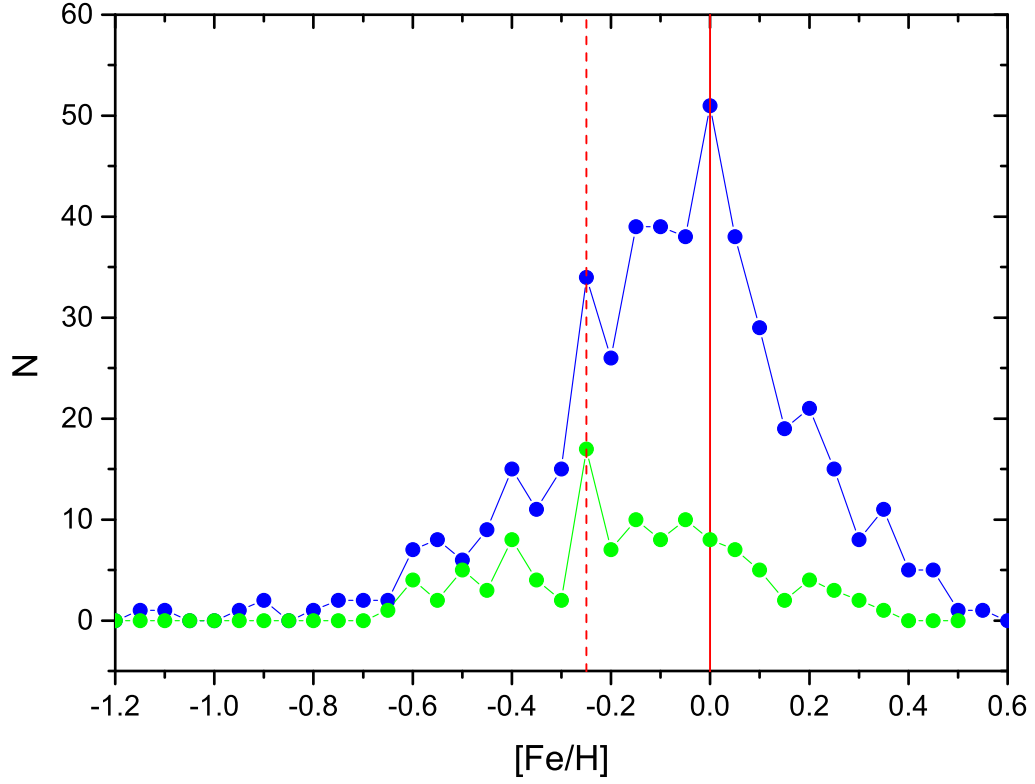


Fig. 6.— Distribution of the metallicity $[\text{Fe}/\text{H}]$ for δ Scuti variables observed by LAMOST. The solid and the dashed lines refer to the two peaks near 0.0 and -0.25, respectively. It is shown that most of the δ Scuti stars have metallicity close to the Sun, i.e., $[\text{Fe}/\text{H}] \sim 0$, while UCVs are more metal poor than the others. Symbols are the same as those in Figs. 4 and 5.

accelerations are higher than the others. The metallicity ($[\text{Fe}/\text{H}]$) distribution is shown in Fig. 6. The peak of the distribution is near $[\text{Fe}/\text{H}] \sim 0$ indicating that most of the δ Scuti variables have metallicity close to that of the Sun. Ten δ Scuti stars have the highest metallicities are shown in Table 5. As those in Figs. 4 and 5, the green dots in Fig. 6 refer to the distribution for UCVs. Its peak is near $[\text{Fe}/\text{H}] \sim -0.25$ reveals that UCVs are more metal poor than the normal δ Scuti stars.

The distribution of the radial velocity (V_r) for those δ Scuti variable stars is displayed in Fig. 7. 698 RVs for 463 δ Scuti variable stars were determined by LAMOST from October 24, 2011 to November 30, 2016 and they are used for constructing the figure. A peak is near $V_r = -10 \text{ km s}^{-1}$ indicating that the V_0 of most variable stars are close to this value. The relation between the pulsating period and the radial velocity is displayed in Fig. 8 where the dashed line refers to the distribution peak of the radial velocity. Those radial velocities of δ Scuti stars are useful to investigate their binarities. It is known that about 60%-80% of field stars in the solar neighbourhood are members of binary or multiple systems (e.g., Duquennoy & Mayor 1991). A very interesting question is how much percent for δ Scuti stars are in binaries or multiples? Gravitational effects of close binary companions may be important to influence the non-radial pulsations through tidal interactions (e.g., Szatmary 1990). In the catalogue published by Rodríguez et al. (2000), 86 δ Scuti stars were pointed out as members of binary or multiple systems. Among 1578 δ Scuti stars in the most recent catalogue published by Chang et al. (2013), 141 cases belong to binaries or multiples. Some of the binary δ Scuti systems were detected by analyzing the light-travel time effect (e.g., Li et al. 2010, 2013; Qian et al. 2015).

Among binary δ Scuti systems, there is an interesting group of eclipsing binaries that are commonly referred to as oEA stars (i.e., oscillating eclipsing systems of Algol type). They are a new class of stellar systems where (B)A-F type primaries are the mass-accreting δ Scuti stars (e.g., Mkrtichian et al. 2002; Liakos et al. 2012). Physical properties of those binary δ Scuti stars were investigated by some investigated (e.g., Mkrtichian et al. 2003; Soydukan et al. 2006; Liakos & Niarchos 2017). Because of the pulsation, the radial-velocity changes should be associated with the light variations of δ Scuti stars. However, the information on the radial velocity is extremely lack. Among the 463 δ Scuti pulsating stars derived spectroscopic parameters, 139 were observed two times or more by LAMOST. The difference between the lowest and the highest radial velocities are determined. 36 δ Scuti stars with V_r difference larger than 15 km s^{-1} are listed in Table 6. The peak-to-peak radial-velocity amplitude for δ Scuti stars is usually less than 10 km s^{-1} (e.g., Breger et al. 1976; Yang & Walker 1986). By considering that the uncertainties for the radial velocity are about 5 km s^{-1} , those δ Scuti stars $\Delta V_r > 15 \text{ km s}^{-1}$ may be the members of binary or multiple systems. Moreover, as shown in Fig. 8, the radial velocities for most δ Scuti stars are around

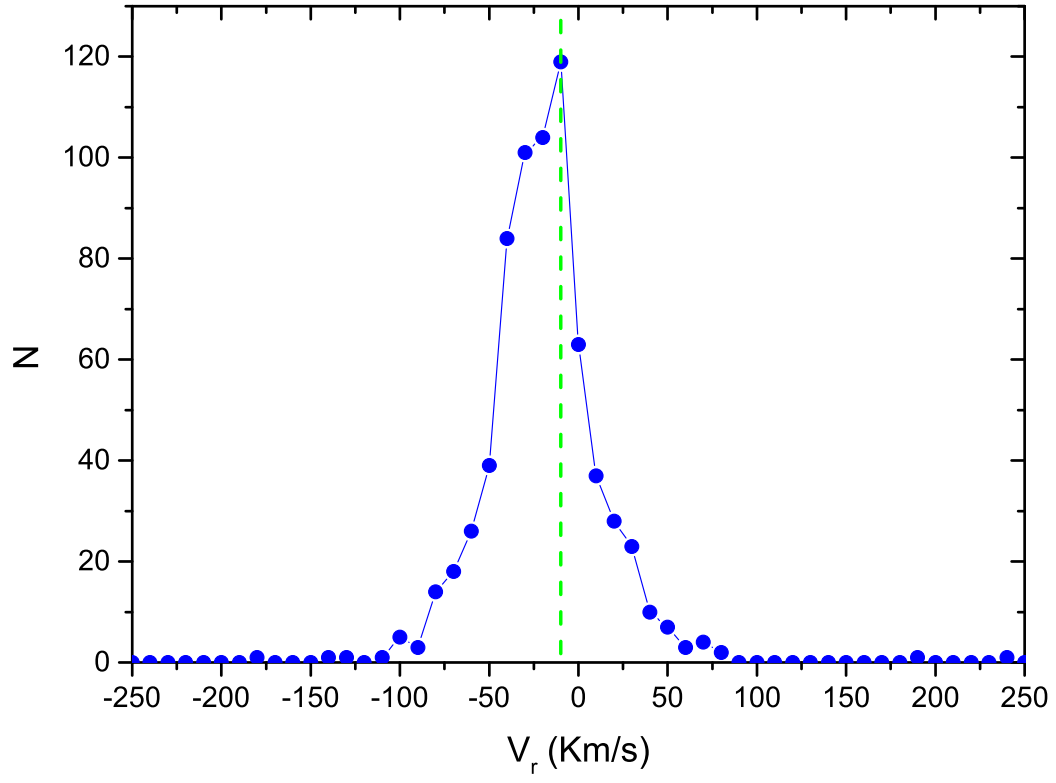


Fig. 7.— Distribution of the radial velocity V_r for δ Scuti pulsating stars observed by LAMOST. There is a peak near $V_r = -10 \text{ km s}^{-1}$.

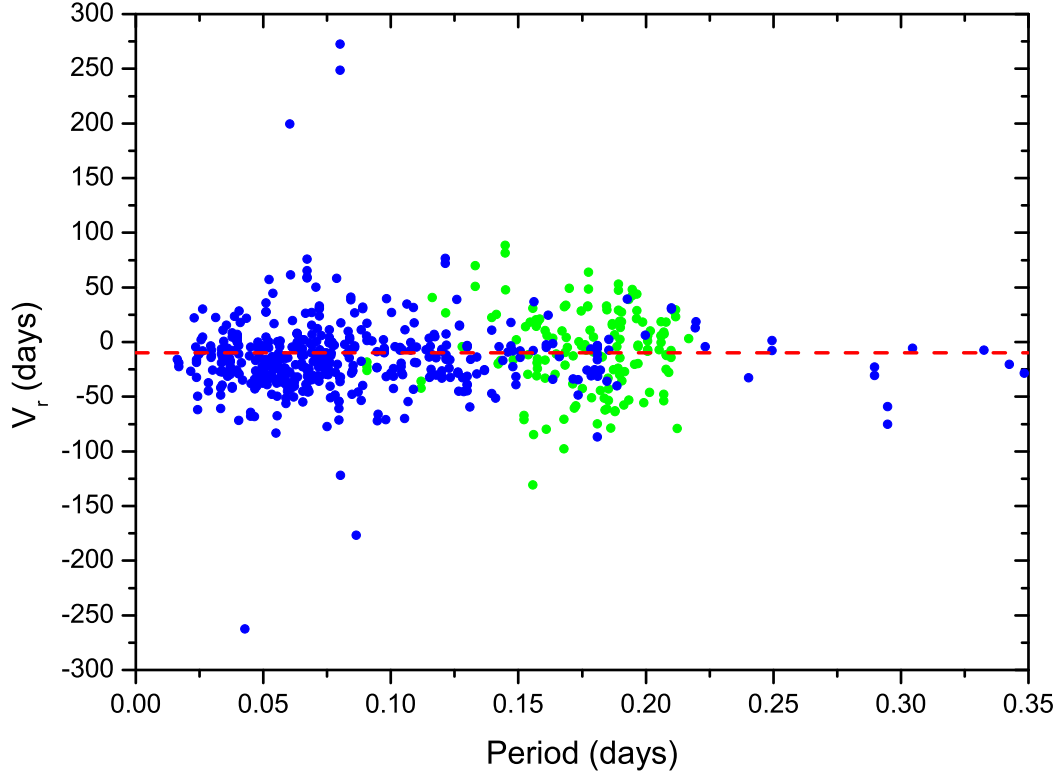


Fig. 8.— The correlation between the radial velocity and the pulsating period. Blue dots refer to NDSTs, while green dots to UCVs (see text for details). The red dashed line represent the peak of the distribution peak of the radial velocity.

$V_r = -10 \text{ km s}^{-1}$. However, the radial velocities of some δ Scuti variables are very high. 28 δ Scuti stars with $V_r > 70 \text{ km s}^{-1}$ are shown in Table 7. They are also candidates of binary δ Scuti systems.

4. Several statistical correlations for normal δ Scuti stars

In this section, we analyze the relationships between those stellar atmospheric parameters (e.g., pulsating period, temperature, gravitational acceleration, metallicity, and amplitude) and then investigate physical properties of the δ Scuti stars. Since the UCVs are quite different from the normal ones. When we investigate the physical properties of NDSTs, they should be excluded. As shown in Fig. 3, there is a good relation between the pulsating period (P) and the effective temperature (T) for NDSTs. A least-squares solution yields,

$$T = 7213.9(\pm 41.6) + 1169.6(\pm 243.3) \exp\left[-\frac{P}{0.035(\pm 0.008)}\right]. \quad (1)$$

This relation (the solid red line) shows that the hotter δ Scuti stars tend to have extremely shorter periods than the late-type variables. It can be explained as an evolutionary effect because the hotter δ Scuti stars tend to be near the main sequence, while cooler variables are more evolved (e.g., Rodríguez et al. 2000).

The correlations between the period and the gravitational acceleration $\log g$ and the metallicity $[\text{Fe}/\text{H}]$ are shown in Figs. 9 and 10 where 10 δ Scuti variable stars without period in VSX are not displayed. Their atmosphere parameters are listed in Table 8. Blue dots in the two figures refers to NDSTs, while the green ones to UCVs. The two dashed lines are the borders of UCVs. It is well known that there is a basic relation for pulsating stars,

$$P\sqrt{\rho/\rho_\odot} = Q, \quad (2)$$

where ρ is the mean density, Q is the pulsation constant. As stars evolving from zero-age main sequence, both the the mean density ρ and the gravitational acceleration $\log g$ should be decreasing. Therefore, the pulsating period should be increasing according to Eq. (2). It is expected that there is a well correlation between the pulsating period and the gravitational acceleration, i.e., the long-period δ Scuti stars have low gravitational accelerations. As shown in Fig. 9, no such relation can be seen if all sample stars are considered. However, after UCVs are excluded, a well relation (the solid red line) between the period and the gravitational acceleration is detected for NDSTs with period shorter than 0.3 days. A least-squares solution leads to the follow equation,

$$\log g = 4.055(\pm 0.016) - 1.286(\pm 0.161) \times P. \quad (3)$$

This relation is a strong observational evidence for the theoretically basic relation for pulsating stars.

The relation between the pulsating period and the metallicity $[\text{Fe}/\text{H}]$ for short-period δ Scuti stars is plotted in Fig. 10. For comparison, those UCVs are also shown in the figure as green dots. For SX Phe-type pulsating stars in the globular clusters, there is a correlation between the metallicities and the periods of the variables (e.g., McNamara 1995, 1997; Rodríguez & Breger 2000). As shown in Fig. 10, the metallicity is weakly correlated with the period (the solid red line). By using the least-squares method, the following equation,

$$[\text{Fe}/\text{H}] = -0.127(\pm 0.028) + 0.99(\pm 0.27) \times P, \quad (4)$$

is derived after UCVs are excluded. The relation tell us that metal-poor stars enter the instability strip mostly with periods shorter than 0.1 days. By using Eq. (4), we could obtain $[\text{Fe}/\text{H}]=0$, when $P=0.128$ days. This indicating that a δ Scuti star with a solar metallicity should has a typical period of $P=0.128$ days. This statistical relation could be explained as that metal-poor pulsating stars evolving into pulsationally unstable states from main sequences displaced below the metal-strong main sequence (e.g., McNamara 1997).

Among the δ Scuti stars catalogued by Chang et al. (2013), 77 of them were observed by LAMOST including 30 UCVs and 47 NDSTs. By using the photometric data in the V-band collected by Chang et al. (2013), the correlation between the period and the photometric amplitude is displayed in Fig. 11 where blue dots refer of NDSTs, while green ones to UCVs. Apart from the variables observed by LAMOST, the other targets investigated by Chang et al. (2013) are also shown as red open circles. As pointed out by Chang et al. (2013), the amplitudes are usually in the range of 0.003-0.9 mag in the V band and this figure tells us that there is no relation between amplitudes and periods for the field stars. Rodríguez & Breger (2001) mentioned that pulsating variables in the period range from 0.25 to 0.3 days may need to be reclassified as evolved Population I δ Scuti or Population II RRc (or γ Dor). As can be seen in Fig. 11, the amplitudes of UCVs are similar to those of NDSTs. The UCVs are solar-type cool variables that have periods in the range from 0.09 to 0.22 days (the two dashed red lines). There are many δ Scuti stars whose pulsating periods are in the period range of UCVs. It is possible that some of them belong to UCVs and they need to be reclassified.

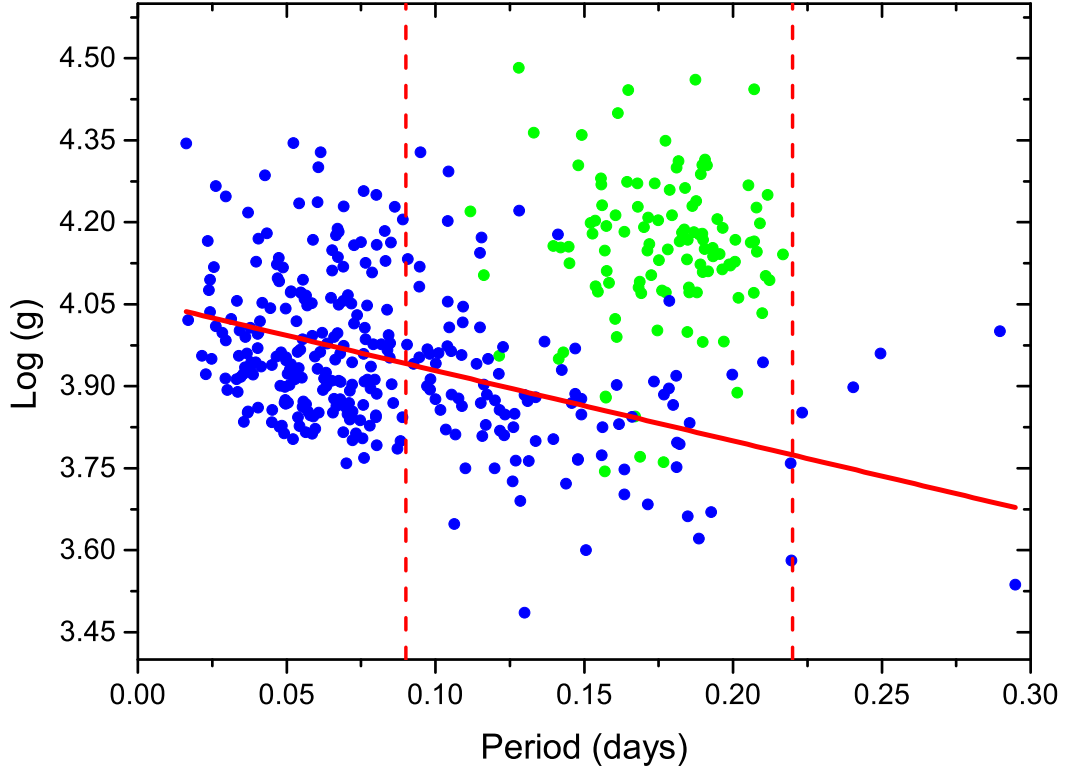


Fig. 9.— The relation between the pulsating period and the gravitational acceleration for short-period NDSTs ($P < 0.3$ days). Blue dots refer of NDSTs, while green ones to UCVs that are between the two red dashed line. The red solid line represents the linear relation between the period and the gravitational acceleration.

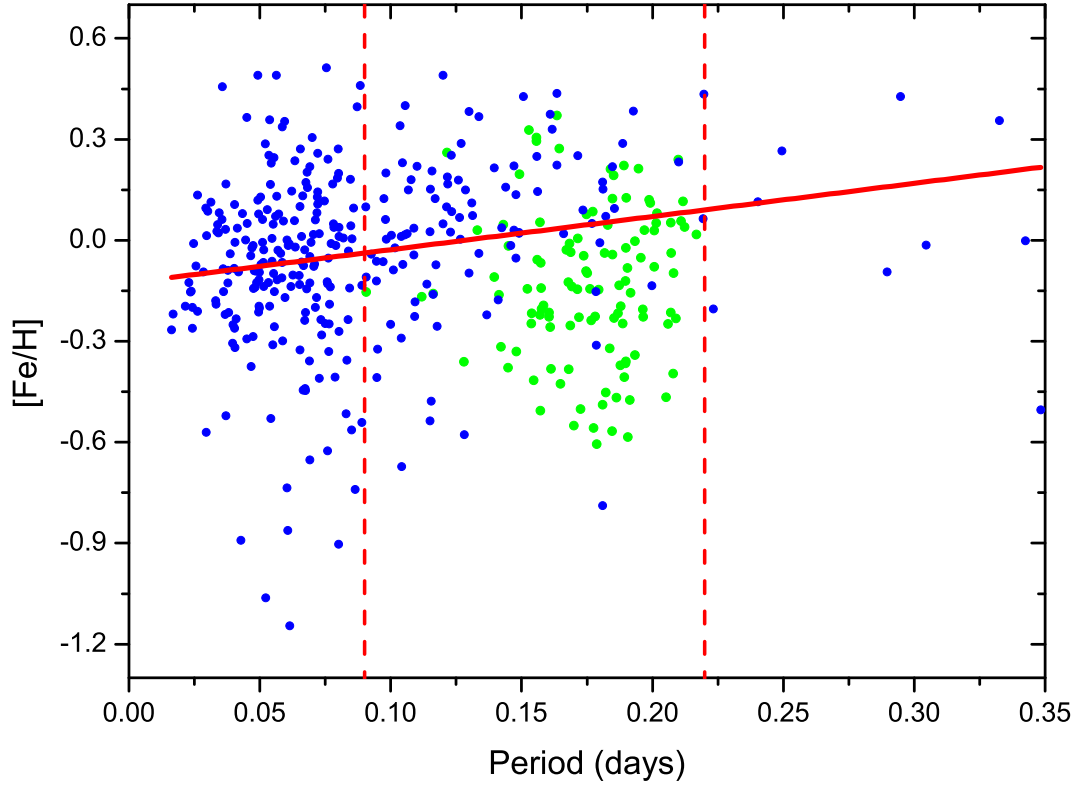


Fig. 10.— The relation between the pulsating period and the metallicity $[Fe/H]$ for short-period δ Scuti variable stars. Symbols are the same as those in Figs. 8 and 9. It shown that there is a linear correlation between the pulsating period and the metallicity.

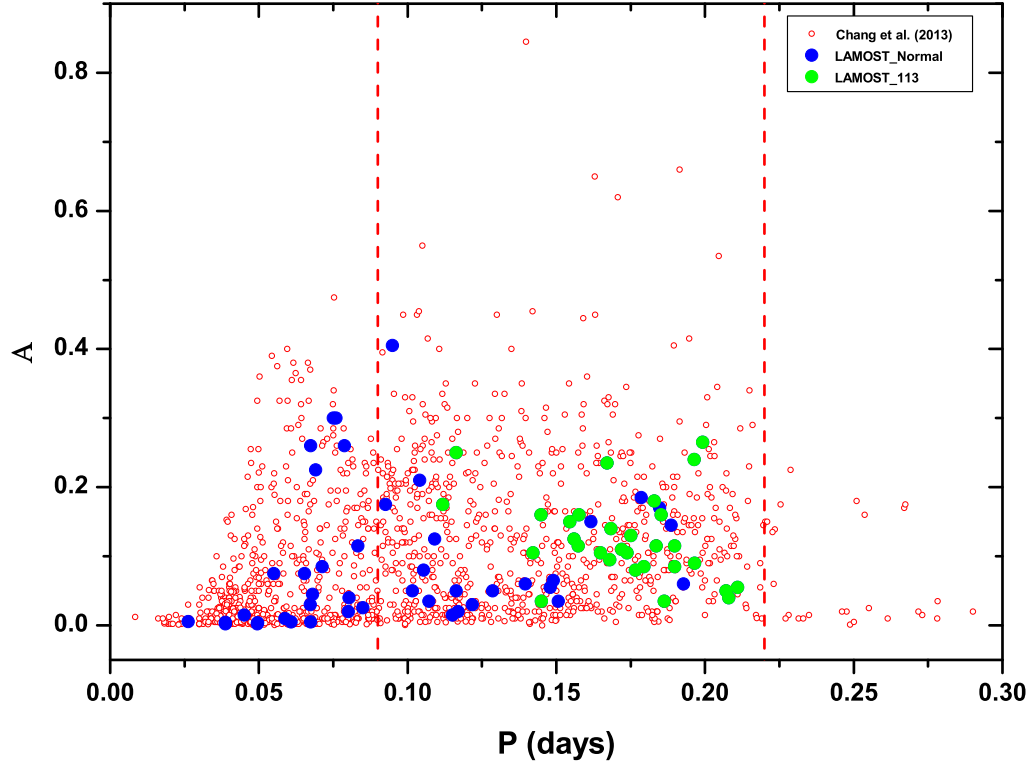


Fig. 11.— The relation between the period and the photometric amplitude (A) for NDSTs and UCVs. Those V-band photometric amplitudes were from Chang et al. (2013). Blue dots refer of NDSTs, while green ones to UCVs. For comparison, the other targets are also shown as red open circles.

5. Discussions and conclusions

In the past twenty years, the number of δ Scuti variable stars is enormously increasing. In addition to the immense effort developed by several photometric surveys on the ground, several space missions such as MOST (Walker et al. 2003), CoRoT (Baglin et al. 2006) and Kepler (Borucki et al. 2010) were carried out that led to the discovery of a lot of new variables and provide high-precision photometry. However, spectroscopic information for those Scuti stars are lack. Among 3688 δ Scuti variables listed in VSX catalogue, 700 of them were observed in LAMOST spectral survey from October 24, 2011 to November 30, 2016. We catalogue those δ Scuti stars and their spectral types are given. Stellar atmospheric parameters for 463 ones are presented. By analyzing 24 δ Scuti variables observed four times or more, we show that the standard errors of the effective temperatures, the gravitational acceleration and the metallicity are usually lower than 50 K, 0.09 dex and 0.06 dex, respectively. Moreover, 352 δ Scuti stars were observed by both Kepler and LAMOST whose effective temperatures have been given in the KIC. By comparing those effective temperatures with the ones determined by LAMOST, it is shown in Fig. 2 that both temperatures for most δ Scuti variables are consistent within 300 K. These results may indicate that stellar atmospheric parameters for δ Scuti stars derived by LAMOST are reliable.

By analyzing stellar atmospheric parameters of δ Scuti pulsating stars derived by LAMOST, we show that there is a group of 113 UCVs with period in the range from 0.09 to 0.23 days. The UCVs are solar-type stars with temperature lower than 6700 K. It is found that there are two peaks on the distributions of the period, the effective temperature, the gravitational acceleration and the the metallicity. One is the main peak, while the other is a small one. We show that the small peaks in those distributions are mainly caused by the existence of this group of variable stars. Those UCVs are more metal poor stars and have higher gravitational accelerations than those of NDSTs.

As shown in Table 6, 36 δ Scuti stars have radial velocity differences larger than 15 km s^{-1} among 139 δ Scuti stars that were observed two times or more by LAMOST. These indicate that they may be candidates of binary δ Scuti systems. Moreover, the radial velocities of some δ Scuti variables are very high. Table 7 shows that 28 δ Scuti variables have radial velocities higher than $V_r = 70 \text{ km s}^{-1}$. They may be also the members of binary or multiple systems. Some of those δ Scuti systems may be eclipsing binaries with high orbital inclinations. If they are real binary systems, the change of the relative distance of the δ Scuti variables from the Sun can result in the observed cyclic change in the O-C (the Observed-Computed maxima times) diagram when the δ Scuti stars orbit the barycenter of the binary system. Therefore, they could be confirmed by monitoring their maxima through the analyses of the light-travel time effect (e.g., Li et al. 2010, 2013; Qian et al. 2015).

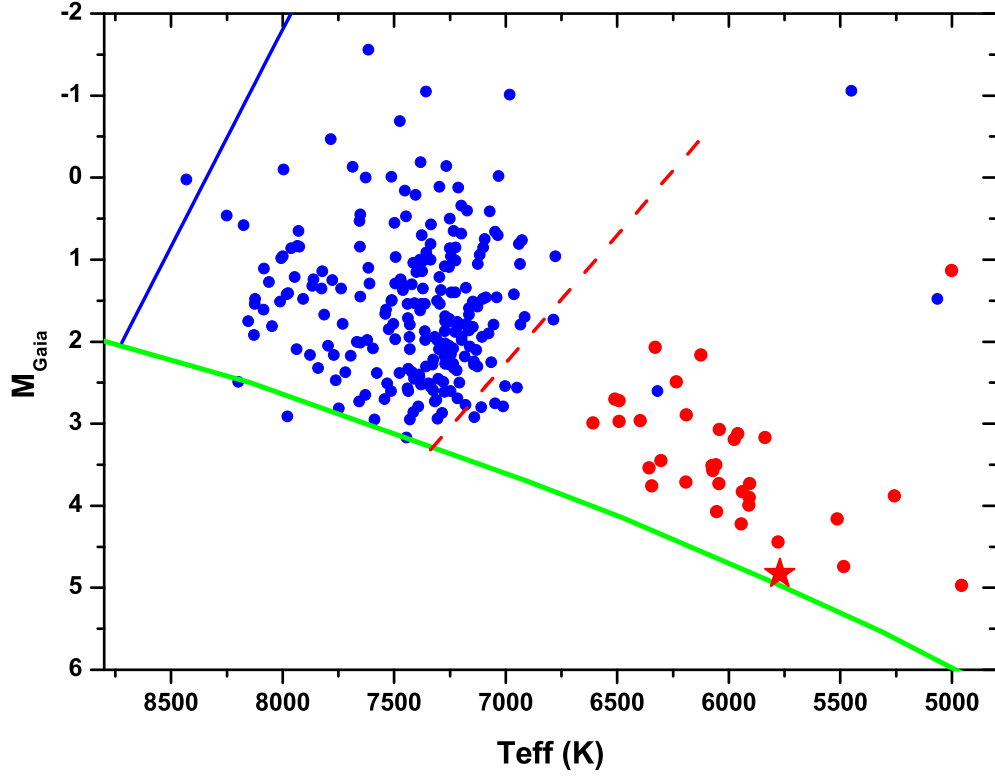


Fig. 12.— The Hertzsprung-Russell diagram for δ Scuti variable stars observed by both LAMOST and GAIA. Blue dots refer to NDSTs, while red dots to UCV ones. The position of the Sun is plotted as the red star. The solid blue line and the red dashed line represent the blue and red edges of δ Scuti variables from McNamara (2000). The green line stands for Zero-age main sequence from Kippenhahn et al. 2012.

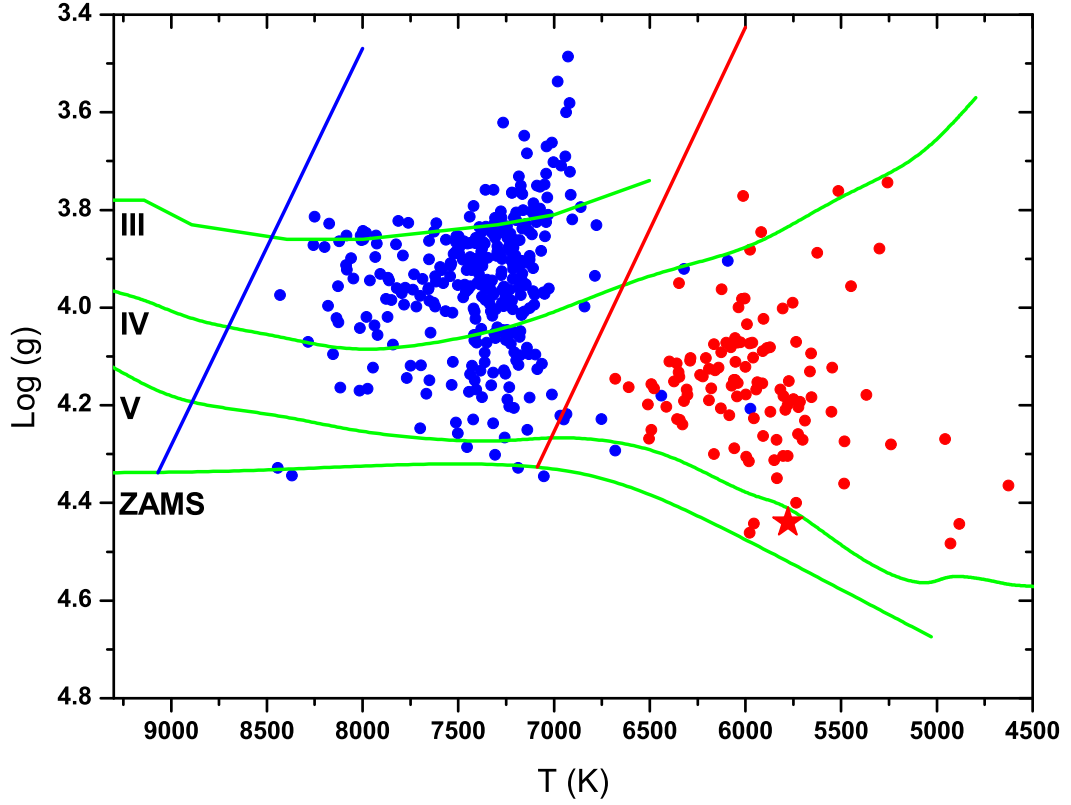


Fig. 13.— The $\log g - T$ diagram for δ Scuti variable stars observed by LAMOST. Symbols are the same as those in Fig 12. The blue and red lines represent the blue and red edges of δ Scuti instability trip from Rodríguez & Breger (2001). The green lines stand for the luminosity classes range between III and V that are from Straizys & Kuriliene (1981), while the zero-age main-sequence line is from Cox (2000).

Among the 463 δ Scuti pulsating stars whose stellar atmospheric parameters were determined by LAMOST, 262 were also observed by Gaia (Gaia Collaboration, Prusti et al. 2016) including 229 NDSTs and 33 UCVs. Their parallaxes and apparent magnitudes were given in Gaia Data Release 1 (Gaia Collaboration, Brown et al. 2016). The H-R diagram of the δ Scuti stars observe by both LAMOST and Gaia is plotted in Fig. 12 where the effective temperature are from LAMOST, while the photometric absolute magnitudes are determined by using Gaia data. The the blue and red edges for δ Scuti stars are from McNamara (2000). The green line in the figure represents the zero-age main sequence from Kippenhahn et al. 2012. As shown in the figure, most of the NDSTs locate inside the classical cepheid instability strip, while the NDSTs are far beyond the red edge of instability strip. It is shown that those UCVs are more evolved than the Sun.

The relations between the gravitational acceleration ($\log g$) and the effective temperature (T) for all variable stars observed by LAMOST is shown in Fig. 13 where blue dots refers to NDSTs, while red dots to UCVs. The position of the Sun is plotted as the red star. The blue and red lines in the figure stand for the borders of δ Scuti pulsating stars. Those green lines shown in the figure represent stellar luminosity classes range between III and V that are from Straizys & Kuriliene (1981), while the zero-age main-sequence line is from Cox (2000). As that shown in the H-R diagram, it is found that all of the UCVs are beyond the red edge of δ Scuti instability trip. They are evolved from zero-age main-sequence stars with luminosity classes range between IV and V. As shown in Figs. 12 and 13, there is a gap between zero-age main sequence and the position of NDSTs in the H-R diagram and in the $\log g - T$ diagram. The gaps increase with growing effective temperature (e.g., Balona & Dziembowski 2011).

Those UCVs should be excluded when we investigate the physical properties of NDSTs because they are quite different from the others. It is found there is a good relation between the effective temperature (T) and the pulsating period (P) for NDSTs. It shows that the temperature is rapidly decreasing when the period is increasing. This relation reveals that the hotter δ Scuti stars tend to be near the main sequence while cooler variables are more evolved (e.g., Rodríguez et al. 2000). A well relation between the gravitational acceleration and the period is discovered for short-period δ Scuti stars with period shorter than 0.3 days (solid red line in Fig. 9). The gravitational acceleration is decreasing as the period increasing. This relation is a direct observational evidence for the theoretically basic relation in Eq. (3) for pulsating stars. Moreover, the metallicity is detected to be weakly correlated with the period as that found for SX Phe-type pulsating stars in the globular clusters (e.g., McNamara 1997).

To check whether those UCVs are δ Scuti stars or not. Their pulsation constants (Q)

are calculated by using the following equation given by Breger (1990),

$$\log(Q/P) = 0.5 \log g + 0.1 M_{bol} + \log T - 6.456. \quad (5)$$

The effective temperature T and the gravitational acceleration $\log g$ are from the data of LAMOST, while M_{bol} could be computed with the equation (e.g., McNamara 2011),

$$M_{bol} = -2.89 \log P - 1.31. \quad (6)$$

The results are shown in Fig. 14 where the dashed red line refers to $Q = 0.033$ days. As displayed in the figure, the values of Q for most of UCVs are larger than 0.033 days. As δ Scuti stars are p-mode and mixed-mode pulsators, Q needs to be below 0.033 day (e.g., Fitch 1981). Therefore, the derived results indicate that most UCVs do not belong to δ Scuti pulsating stars. The other method to check them is to determine the ratios of radial velocity to light amplitude of the stellar variability. If they are δ Scuti pulsating stars, the ratios should be in the range from 40 to 120 km/s/mag (e.g., e.g., Breger et al. 1976; Daszynska-Daszkiewicz et al. 2005). 28 UCVs were observed two times or more and the difference between the lowest and the highest radial velocities are determined. Then the ratios of radial velocity to light amplitude could be estimated and the results are plotted in Fig. 15. As shown in the figure, although some ratios are below 40 km/s/mag, we could not rule out them as δ Scuti stars because our data are insufficient to derive the amplitude of the radial velocity curve.

As shown in Table 2, some UCVs are classified as both δ Scuti stars (DSCT) and EC-type contact binaries implying that many are actually suspected contact binaries, i.e. their variability classification is not unique. Those suspected contact binary stars have double periods, i.e., in the period range from 0.18 to 0.44 days. This is typical range for EW-type contact binary systems (see Fig. 1 in Qian et al. 2017). Those binary stars are similar to contact systems investigated by Qian et al. (2007, 2013, 2014). Moreover, as listed in Table 7, several UCVs show large radial velocity scatters indicating that they may be close binary stars. In this way, the derived effective temperatures for those sample stars are very useful during solving their light curves. The other atmospheric parameters (e.g., $\log g$ and $[\text{Fe}/\text{H}]$) will provide us valuable information to understand their formation and evolutionary state. Our results show that about 24.4% of the known δ Scuti pulsating stars were misclassified. They may be close binary stars rather than δ Scuti stars. As shown in Fig. 1, about 1800 objects listed in VSX are classified as δ Scuti pulsating stars in the period range from 0.09 to 0.22 days. Some of them may need to be reclassified.

The blue edge of the instability strip for δ Scuti stars is theoretically well constrained (e.g., Pamyatnykh 2000). However, the red edge is rather complicated and has a large range of possibilities for the slope and shape (e.g., Chang et al. 2013). The investigation

of some authors (e.g., Houdek et al. 1999) indicated that oscillations in solar-like stars are intrinsically damped and stochastically driven by convection, while the calculations by Cheng & Xiong (1997) using the theory of Xiong (1989) predicted over stable solar oscillations. If some UCVs are confirmed as pulsating stars, they may be a new-type pulsators. Their observations and investigations will shed light on theoretical instability domains and on the theories of interacting between the pulsation and the convection of solar-type stars. New observations and detailed investigations on UCVs are timely and required urgently in the near future.

This work is partly supported by National Natural Science Foundation of China (No. 11325315). Guoshoujing Telescope (the Large Sky Area Multi-Object Fiber Spectroscopic Telescope LAMOST) is a National Major Scientific Project built by the Chinese Academy of Sciences. Funding for the project has been provided by the National Development and Reform Commission. LAMOST is operated and managed by the National Astronomical Observatories, Chinese Academy of Sciences. Spectroscopic observations used in the paper were obtained with LAMOST from October 24, 2011 to November 30, 2016. This work has made use of data from the European Space Agency (ESA) mission *Gaia* (<https://www.cosmos.esa.int/gaia>), processed by the *Gaia* Data Processing and Analysis Consortium (DPAC, <https://www.cosmos.esa.int/web/gaia/dpac/consortium>). Funding for the DPAC has been provided by national institutions, in particular the institutions participating in the *Gaia* Multilateral Agreement.

REFERENCES

- Baglin, A., Auvergne, M., Barge, P., et al., 2006, in The CoRoT Mission, Pre-Launch Status, Stellar Seismology and Planet Finding, ed. M. Fridlund, A. Baglin, J. Lochard, & L. Conroy, ESA Publications Division, Noordwijk, Netherlands, ESA SP-1306, 33
- Balona, L. A. & Dziembowski, W. A., 2011, MNRAS, 417, 591
- Borucki, W. J., Koch, D., Basri, G., Batalha, N., Brown, T., Caldwell, D., Caldwell, J., et al. 2010, Science, 327, 977
- Breger, M., 1979, PASP, 91, 5
- Breger, M., 1990, DSSN, 2, 13
- Breger, M., 2000, in ASP Conf. Ser. 210, Delta Scuti and Related Stars, ed. M. Breger, & M. Montgomery (San Francisco, CA: ASP), 3
- Breger, M., Hutchins, J., Kuhl, L. V., 1976, ApJ, 210, 163

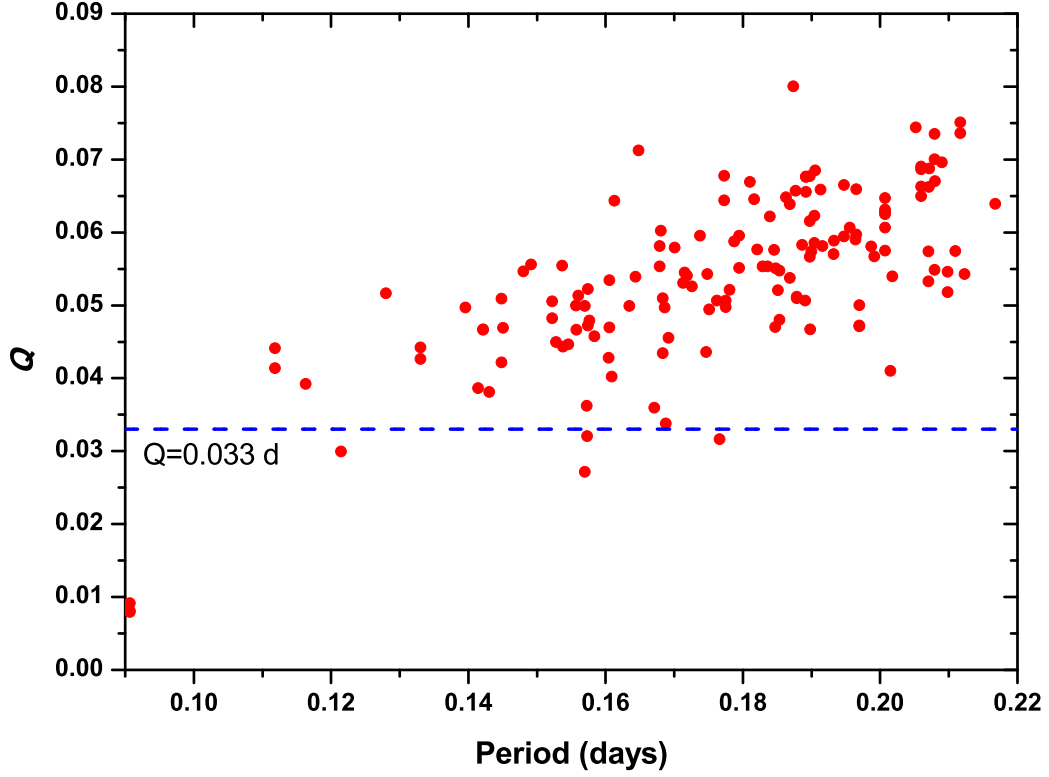


Fig. 14.— The plot of the pulsation constant (Q) along with the period for the UCVs observed by LAMOST. The dashed red line refers to $Q = 0.033$ days. It is shown the values of Q for most of UCVs are larger than 0.033 days indicating that they may not be δ Scuti pulsating stars.

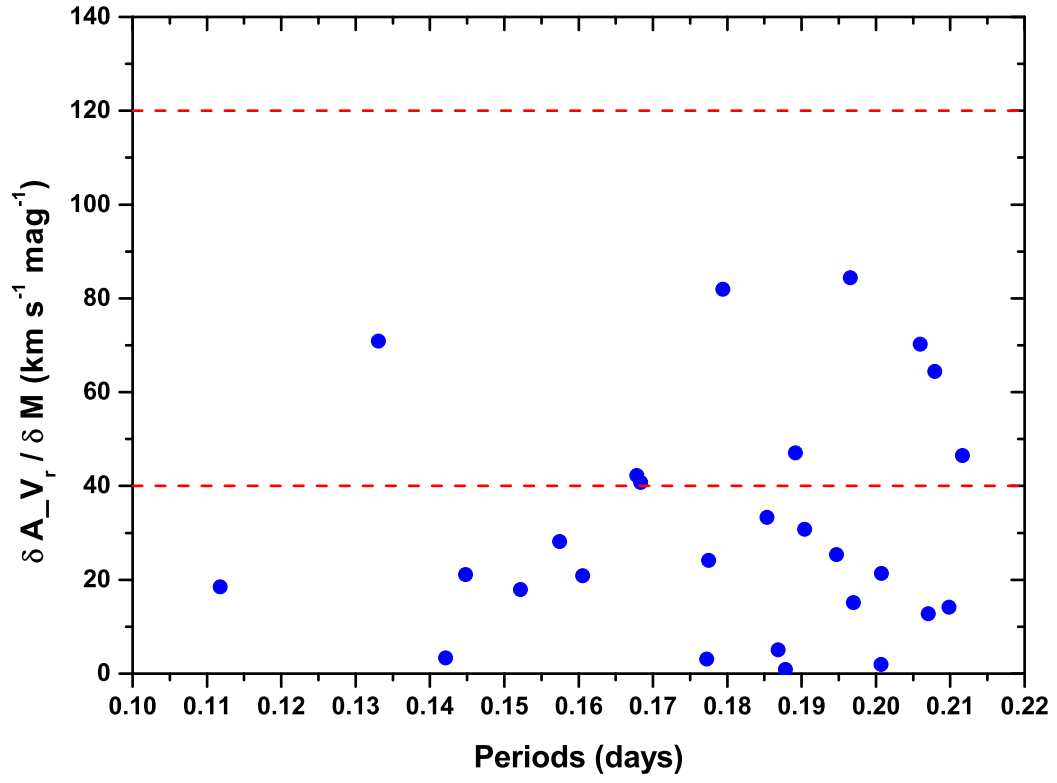


Fig. 15.— A plot of the ratio of radial velocity to light amplitude along with the period for 28 UCVs observed two times or more. The two red dashed lines refer to the range for δ Scuti stars.

- Breger, M., Lenz, P., Antoci, V., Guggenberger, E., Shobbrook, R. R., Handler, G., Ngwato, B., Rodler, F., et al., 2005, *A&A*, 435, 955
- Chang, S.-W., Protopapas, P., Kim, D.-W., Byun, Y.-I., 2013, *AJ*, 145, 132
- Cheng Q.-L. & Xiong D.-R., 1997, *A&A*, 319, 981
- Cox, A. N., 2000, *Allen’s Astrophysical Quantities*, 4th ed. (New York: Springer), P.381
- Cui, X. Q., Zhao, Y. H., Chu, Y. Q., et al. 2012, *RAA*, 12, 1197
- Daszyńska-Daszkiewicz, J., Dziembowski, W. A., Pamyatnykh, A. A., Breger, M., Zima, W., Houdek, G., 2005, *A&A*, 438, 653
- Duquennoy A. & Mayor M., 1991, *A&A*, 248, 485
- Fitch, W. S., 1981, *ApJ*, 249, 218
- Gaia Collaboration, Brown, A. G. A., Vallenari, A., et al., 2016, *A&A*, 595, A2
- Gaia Collaboration, Prusti, T., de Bruijne, J. H. J., et al., 2016, *A&A*, 595, A1
- Gao, H., Zhang, H.-W., Xiang, M.-S., et al., 2015, *RAA*, 15, 2204
- Gautschy, A. & Saio, H. 1995, *ARA&A*, 33, 75
- Houdek, G., Balmforth, N. J., Christensen-Dalsgaard, J., Gough, D. O., 1999, *A&A*, 351, 582
- Kippenhahn, R., Weigert, A., Weiss, A., 2012, *Stellar Structure and Evolution*, Springer-Verlag Berlin Heidelberg
- Koleva, M., Prugniel, P., Bouchard, A. & Wu, Y. 2009, *A&A*, 501, 1269
- Lopez de Coca, P., Rolland, A., Rodríguez, E., Garrido, R., 1990, *A&AS*, 83, 51
- Li L.-J., Qian S.-B., Xiang F.-Y., 2010, *PASJ*, 62, 987
- Li L.-J., Qian S.-B., 2013, *PASJ*, 65
- Liakos A. & Niarchos P., 2017, *MNRAS*, 465, 1181
- Liakos A., Niarchos P., Soydugan E., Zasche P., 2012, *MNRAS*, 422, 1250
- Luo, A.-L., Zhao, Y.-H., Zhao, G., et al. 2015, *RAA*, 15, 1095
- McNamara, D. H., 1995, *AJ*, 109, 1751
- McNamara, D. H., 1997, *PASP*, 109, 1221
- McNamara, D. H., 2000, *ASPC*, 210, 373
- McNamara, D. H., 2011, *AJ*, 142, 110
- Mkrtychian D. E., Kusakina A. V., Gamarova A. Y., Nazarenko V., 2002, *ASP Conf. Ser.* Vol. 259, P. 96

- Mkrtichian D. E. et al., 2003, ASP Conf. Ser. Vol. 292, P. 113
- Palaversa, L., Ivezić, Ž., Eyer, L., Ruzdjak, D., Sudar, D., Galin, M., Kroffin, A., et al., 2013, AJ, 146, 101
- Pamyatnykh A. A., 2000, in ASP Conf. Ser. 210, Delta Scuti and Related Stars, ed. M. Breger, & M. Montgomery (San Francisco, CA: ASP), 215
- Pojmanski, G., 1997, AcA, 47 467
- Pojmanski, G., Pilecki, B., and Szczygiel, D., 2005, AcA, 55, 275
- Prugniel, P. & Soubiran, C. 2001, A&A, 369, 1048
- Qian, S.-B., He, J.-J., Zhang, J., Zhu, L.-Y., Shi, X.-D., Zhao, E.-G., Zhou, X., 2017a, arXiv170503996Q
- Qian, S.-B., Li, L.-J., Wang, S.-M., He, J.-J., Zhou, X., Jiang, L.-Q., 2015, AJ, 149, 4
- Qian, S.-B., Liu, N.-P., Li, K., He, J.-J., Zhu, L.-Y., Zhao, E. G., Wang, J.-J., Li, L.-J., & Jiang, L.-Q., 2013, ApJS, 209, 13
- Qian, S.-B., Wang, J.-J., Zhu, L.-Y., Snoonthornthum, B., Wang, L.-Z., Zhao, E.-G.; Zhou, X., Liao, W.-P., Liu, N.-P., 2014, ApJS, 212, 4
- Qian, S.-B., Yuan, J.-Z., Snoonthornthum, B., Zhu, L.-Y., He, J.-J., Yang, Y.-G., 2007, ApJ, 671, 811
- Rodríguez, E. & Breger, M., 2001, A&A, 366, 178
- Rodríguez, E., López-González, M. J., López de Coca, P., 2000, A&AS, 144, 469
- Rodríguez, E. & López-González, M. J., 2000, A&A, 359, 597
- Samus, N. N., Kazarovets, E. V., Durlevich, O. V., Kireeva, N. N., Pastukhova, E. N., 2017, General Catalogue of Variable Stars: new version. GCVS 5.1 (the first stage of the fifth edition), ARep, 60, No. 80
- Soydugan E., İbanoğlu C., Soydugan F., Akan M. C., Demircan O., 2006, MNRAS, 366, 1289
- Straizys, V. & Kuriliene, G., 1981, Ap&SS, 80, 353
- Szatmary, K., 1990, JAVSO, 19, 52
- Szczygiel, D. M. & Fabrycky, D. C., 2007, MNRAS, 377, 1263
- Walker, G., Matthews, J., Kuschnig, R., et al. 2003, PASP, 115, 1023
- Wang, S.-G., Su, D.-Q., Chu, Y.-Q., et al. 1996, Appl. Opt., 35, 5155
- Watson, C. L., 2006, Society for Astronomical Sciences Annual Symposium, 25, 47

- Woźniak, P. R., Vestrand, W. T., Akerlof, C. W., Balsano, R., Bloch, J., Casperson, D., Fletcher, S., et al., 2004, *AJ*, 127, 2436
- Wu, Y., Singh, H. P., Prugniel, P., Gupta, R., & Koleva, M. 2011, *A&A*, 525, A71
- Wu, Y., Du, B., Luo, A., Zhao, Y., & Yuan, H. 2014, *Statistical Challenges in 21st Century Cosmology*, IAU Symposium, 306, 340
- Yang, S. & Walker, G. A. H., 1986, *PASP*, 98, 862
- Uytterhoeven, K., Moya, A., Grigahcène, A., Guzik, J. A., Gutiérrez-Soto, J., Smalley, B., et al., 2011, *A&A*, 534, A125
- Xiong D.-R., 1989, *A&A*, 254, 362
- Xiong D.-R. & Deng L., 2001, *MNRAS*, 324, 243
- Zhao, G., Zhao, Y.-H., Chu, Y.-Q., et al. 2012, *RAA*, 12, 723

Table 2: Stellar atmospheric parameters for the 113 UCVs detected by LAMOST (the first 50 lines of the whole table).

| Name | R.A. (deg) | Dec. (deg) | Type | Period (days) | Dist | Date | Sp. | T (K) | E_1 | $\log g$ | E_2 | [Fe/H] | E_3 | V_T (km s ⁻¹) | E_4 |
|---------------------|------------|------------|-----------------|---------------|-------|------------|-----|---------|--------|----------|-------|--------|-------|-----------------------------|-------|
| GM Com | 183.1038 | 27.38008 | DSCTC | 0.208 | 0.177 | 2011-12-21 | F3 | 6679.86 | 16.45 | 4.146 | 0.022 | -0.097 | 0.016 | -12.37 | 2.07 |
| ASAS J001921+0127.1 | 4.83683 | 1.45297 | DSCT—EC—ESD | 0.156951 | 0.087 | 2012-10-29 | G7 | 5257.5 | 21.51 | 3.744 | 0.03 | 0.054 | 0.02 | 14.26 | 1.87 |
| ASAS J010045+2648.4 | 15.18808 | 26.80683 | DSCT—EC—ESD | 0.190532 | 0.029 | 2015-10-31 | F2 | 5981.42 | 1.98 | 4.315 | 0.001 | -0.585 | 0.002 | -35.52 | 0.44 |
| ASAS J011159+2548.8 | 17.99496 | 25.81331 | DSCT—EC—ESD | 0.157222 | 0.049 | 2014-10-25 | F6 | 5975.66 | 286.63 | 3.881 | 0.411 | -0.506 | 0.266 | -30.82 | 21.25 |
| ASAS J011208+0217.2 | 18.03254 | 2.28617 | DSCT | 0.176614 | 0.019 | 2012-10-31 | G3 | 5514.19 | 35.68 | 3.761 | 0.051 | -0.238 | 0.033 | -7.5 | 2.99 |
| ASAS J011959+1500.4 | 19.99579 | 15.00731 | DSCT | 0.199153 | 0.036 | 2016-01-19 | F9 | 6000.16 | 12.95 | 4.121 | 0.017 | 0.111 | 0.012 | -55.62 | 1.57 |
| ASAS J012334+2108.6 | 20.89288 | 21.14336 | DSCT | 0.185343 | 0.075 | 2012-12-03 | F2 | 6006.9 | 55.41 | 4.02 | 0.078 | -0.244 | 0.052 | -53.55 | 4.75 |
| ASAS J012334+2108.6 | 20.89288 | 21.14336 | DSCT | 0.185343 | 0.075 | 2014-11-19 | F6 | 6079.87 | 137.39 | 4.123 | 0.196 | -0.219 | 0.128 | -42.88 | 10.97 |
| ASAS J013458+0553.2 | 23.74217 | 5.88589 | DSCT | 0.164786 | 0.063 | 2015-12-11 | F9 | 5956.97 | 313.27 | 4.442 | 0.449 | -0.426 | 0.291 | -11.05 | 23.31 |
| ASAS J022414+2741.6 | 36.05646 | 27.69336 | DSCT | 0.155998 | 0.026 | 2013-10-06 | G3 | 5688.79 | 22.41 | 4.231 | 0.031 | -0.058 | 0.021 | -84.62 | 2.4 |
| ASAS J030054+2301.7 | 45.22333 | 23.02756 | DSCT—EC | 0.181652 | 0.017 | 2015-10-30 | G2 | 5850.71 | 80.55 | 4.312 | 0.115 | -0.038 | 0.075 | -12.15 | 6.39 |
| ASAS J030701+1534.2 | 46.75504 | 15.56981 | DSCT—EC | 0.171276 | 0.026 | 2012-09-30 | F2 | 6055.37 | 12.61 | 4.148 | 0.017 | -0.146 | 0.012 | -38.42 | 1.43 |
| ASAS J032314+0406.0 | 50.80875 | 4.10236 | DSCT | 0.157606 | 0.072 | 2014-12-02 | F2 | 6052.06 | 98.27 | 4.111 | 0.14 | -0.204 | 0.092 | 18.5 | 7.79 |
| ASAS J035613+2600.1 | 59.05558 | 26.00178 | DSCT—EC | 0.195533 | 0.058 | 2016-11-10 | F5 | 6345.77 | 2.41 | 4.142 | 0.001 | -0.052 | 0.002 | -20.27 | 0.54 |
| ASAS J040216-0321.7 | 60.56533 | -3.36314 | DSCT—EC—ESD | 0.155724 | 0.018 | 2012-11-01 | K3 | 4956.91 | 56.51 | 4.269 | 0.078 | 0.305 | 0.053 | 30.99 | 5.7 |
| ASAS J041458+0501.2 | 63.7415 | 5.01972 | DSCT—EC | 0.170028 | 0.024 | 2015-11-29 | F0 | 6320.95 | 3.08 | 4.191 | 0.003 | -0.551 | 0.003 | 49.05 | 0.63 |
| ASAS J052412+0020.2 | 81.05208 | 0.33606 | DSCT | 0.196369 | 0.018 | 2014-11-18 | F5 | 6358.69 | 10.81 | 4.114 | 0.015 | -0.205 | 0.01 | 21.57 | 1.21 |
| ASAS J053125+1103.8 | 82.85413 | 11.06303 | DSCT | 0.144799 | 0.041 | 2014-12-10 | F8 | 5857.76 | 10.94 | 4.081 | 0.015 | -0.428 | 0.01 | 81.63 | 1.14 |
| ASAS J053125+1103.8 | 82.85413 | 11.06303 | DSCT | 0.144799 | 0.374 | 2013-10-02 | F2 | 5966.68 | 2.08 | 4.229 | 0.001 | -0.33 | 0.002 | 88.38 | 0.51 |
| ASAS J060036+2533.1 | 90.1485 | 25.55186 | DSCT—EC | 0.16044 | 0.3 | 2013-01-29 | F9 | 5906.02 | 17.77 | 4.023 | 0.025 | -0.227 | 0.017 | 10.7 | 1.77 |
| ASAS J062150+2026.7 | 95.45875 | 20.44475 | DSCT—EC—ESD | 0.141396 | 0.051 | 2012-03-06 | F5 | 6347.37 | 123.78 | 3.95 | 0.177 | -0.162 | 0.115 | 25.46 | 9.3 |
| ASAS J063122+0050.8 | 97.84071 | 0.84717 | DSCT—EC—ESD | 0.191597 | 0.049 | 2013-01-03 | F5 | 6398.08 | 4.24 | 4.11 | 0.005 | -0.156 | 0.004 | -27.09 | 0.8 |
| ASAS J063713-0234.6 | 99.30292 | -2.57678 | DSCT—EC | 0.158359 | 0.058 | 2014-11-19 | G2 | 5910.64 | 25.39 | 4.089 | 0.035 | -0.194 | 0.024 | 21.06 | 2.38 |
| ASAS J064626+2629.8 | 101.6081 | 26.49736 | DSCT—EC | 0.205972 | 0.137 | 2014-03-06 | F0 | 6596.39 | 1.76 | 4.153 | 0.001 | -0.24 | 0.001 | 5.55 | 0.39 |
| ASAS J064626+2629.8 | 101.6081 | 26.49736 | DSCT—EC | 0.205972 | 0.137 | 2012-03-11 | F2 | 6607.35 | 224.43 | 4.182 | 0.321 | -0.25 | 0.209 | 5.8 | 16.97 |
| ASAS J064626+2629.8 | 101.6081 | 26.49736 | DSCT—EC | 0.205972 | 0.078 | 2015-01-12 | F0 | 6615.3 | 2.33 | 4.133 | 0.002 | -0.249 | 0.002 | 18.51 | 0.58 |
| ASAS J064626+2629.8 | 101.6081 | 26.49736 | DSCT—EC | 0.205972 | 0.078 | 2016-01-18 | F2 | 6619.5 | 5.56 | 4.185 | 0.006 | -0.257 | 0.005 | -0.46 | 1.05 |
| ASAS J070051+0113.4 | 105.2115 | 1.22522 | DSCT—EC | 0.174814 | 0.086 | 2014-10-21 | G7 | 5724.1 | 16.79 | 4.204 | 0.023 | 0.077 | 0.016 | -3.36 | 1.84 |
| ASAS J071025+2728.2 | 107.6047 | 27.47008 | DSCT | 0.168026 | 0.085 | 2013-03-13 | F5 | 6356.82 | 1.87 | 4.228 | 0.001 | -0.383 | 0.002 | 32.35 | 0.41 |
| ASAS J071540+2022.2 | 108.9157 | 20.37111 | DSCT—EC | 0.200724 | 0.105 | 2013-11-14 | F5 | 6301.7 | 4.38 | 4.158 | 0.005 | -0.064 | 0.004 | -8.5 | 0.82 |
| ASAS J071540+2022.2 | 108.9157 | 20.37111 | DSCT—EC | 0.200724 | 0.105 | 2013-11-24 | F5 | 6305.5 | 9.22 | 4.161 | 0.012 | -0.076 | 0.009 | -6.94 | 1.21 |
| ASAS J071540+2022.2 | 108.9157 | 20.37111 | DSCT—EC | 0.200724 | 0.105 | 2013-11-14 | F5 | 6307.57 | 6.19 | 4.187 | 0.008 | -0.08 | 0.006 | 0.92 | 0.9 |
| ASAS J071540+2022.2 | 108.9157 | 20.37111 | DSCT—EC | 0.200724 | 0.105 | 2013-11-24 | F5 | 6312.11 | 17.3 | 4.165 | 0.024 | -0.096 | 0.016 | -6.89 | 1.8 |
| ASAS J071838+2819.9 | 109.6582 | 28.33111 | DSCT | 0.11179 | 0.039 | 2015-03-03 | F6 | 6075.92 | 21.2 | 4.193 | 0.029 | -0.19 | 0.02 | -35.74 | 2.07 |
| ASAS J071838+2819.9 | 109.6582 | 28.33111 | DSCT | 0.11179 | 0.476 | 2014-12-18 | F7 | 6094.49 | 11.23 | 4.246 | 0.015 | -0.147 | 0.011 | -42.23 | 1.31 |
| ASAS J071912+2102.9 | 109.8019 | 21.04772 | DSCT—EC—ESD | 0.186852 | 0.24 | 2013-11-24 | F9 | 5969.29 | 155.28 | 4.118 | 0.222 | -0.334 | 0.145 | 16.7 | 12.13 |
| ASAS J071912+2102.9 | 109.8019 | 21.04772 | DSCT—EC—ESD | 0.186852 | 0.24 | 2013-11-14 | F2 | 6119.37 | 2.7 | 4.246 | 0.002 | -0.099 | 0.002 | 15.58 | 0.59 |
| ASAS J073122+1556.0 | 112.842 | 15.93331 | DSCT | 0.20712 | 0.077 | 2016-03-20 | K3 | 4883.19 | 8.67 | 4.443 | 0.005 | -0.038 | 0.007 | 7.28 | 1.9 |
| ASAS J075218+0812.1 | 118.0764 | 8.20033 | DSCT—EC | 0.169149 | 0.021 | 2013-02-14 | G3 | 5735.5 | 160.51 | 4.07 | 0.23 | -0.137 | 0.149 | -4.75 | 11.93 |
| ASAS J075428+1407.8 | 118.618 | 14.13039 | DSCT—EC | 0.189175 | 0.053 | 2013-02-15 | F7 | 5995.43 | 35.68 | 4.306 | 0.05 | -0.396 | 0.034 | 53.03 | 3.32 |
| ASAS J075428+1407.8 | 118.618 | 14.13039 | DSCT—EC | 0.189175 | 0.053 | 2013-12-14 | F7 | 6079.52 | 16.23 | 4.294 | 0.022 | -0.413 | 0.015 | 29.01 | 1.73 |
| ASAS J075428+1407.8 | 118.618 | 14.13039 | DSCT—EC | 0.189175 | 0.053 | 2013-12-14 | F6 | 6101.64 | 25.2 | 4.264 | 0.035 | -0.409 | 0.024 | 47.56 | 2.54 |
| ASAS J081832-0817.2 | 124.6333 | -8.28717 | DSCT | 0.173738 | 0.087 | 2012-12-23 | G3 | 5837.16 | 50.34 | 4.271 | 0.071 | -0.046 | 0.047 | 0.35 | 4.39 |
| ASAS J082116+0301.1 | 125.3164 | 3.01819 | DSCT—EC—ESD | 0.184513 | 0.056 | 2015-03-22 | F3 | 6350.3 | 3.77 | 4.132 | 0.004 | -0.567 | 0.004 | 33.15 | 0.81 |
| ASAS J082400-0035.9 | 125.999 | -0.59797 | DSCT—EC | 0.207058 | 0.036 | 2013-11-25 | F4 | 6478.66 | 2.85 | 4.165 | 0.002 | -0.215 | 0.002 | 9.06 | 0.72 |
| ASAS J083349+0253.7 | 128.4553 | 2.89439 | DSCT—RRC—EC—ESD | 0.211647 | 0.047 | 2013-03-28 | F5 | 6488.31 | 2.83 | 4.242 | 0.003 | 0.119 | 0.003 | 23.35 | 0.6 |
| ASAS J083349+0253.7 | 128.4553 | 2.89439 | DSCT—RRC—EC—ESD | 0.211647 | 0.043 | 2015-03-22 | F5 | 6495.78 | 2.84 | 4.258 | 0.002 | 0.114 | 0.003 | 29.4 | 0.71 |
| ASAS J083952+0052.4 | 129.9679 | 0.87256 | DSCT—EC—ESD | 0.133043 | 0.529 | 2013-03-24 | K5 | 4551.25 | 90.86 | 4.362 | 0.13 | 0.035 | 0.084 | 70.01 | 6.79 |
| ASAS J083952+0052.4 | 129.9679 | 0.87256 | DSCT—EC—ESD | 0.133043 | 0.529 | 2013-03-24 | K4 | 4702.68 | 55.61 | 4.365 | 0.08 | 0.024 | 0.052 | 50.87 | 4.14 |
| ASAS J084358+1328.1 | 130.9916 | 13.46969 | DSCT—EC | 0.17725 | 0.066 | 2015-10-31 | G3 | 5818.06 | 2.58 | 4.33 | 0.002 | 0.077 | 0.002 | 32.38 | 0.62 |

Table 3: Catalogue of NDSTs observed by LAMOST (the first 50 observations).

| Name | R.A. (deg) | Dec. (deg) | Type | Period (days) | Dist. | Date | Sp. | T (K) | E_1 | $\log g$ | E_2 | [Fe/H] | E_3 | V_t (km s $^{-1}$) | E_4 |
|---------------------|------------|------------|---------------------|---------------|-------|------------|------|---------|--------|----------|-------|--------|-------|-----------------------|-------|
| GP And | 13.82563 | 23.16372 | DSCT | 0.078683 | 0.125 | 2013-10-15 | F0 | 7197.81 | 39.33 | 4.108 | 0.055 | -0.407 | 0.037 | 58.31 | 3.52 |
| YZ Boo | 231.02917 | 36.86683 | DSCT | 0.104092 | 0.026 | 2015-02-18 | A6IV | 7165.39 | 11.92 | 4.057 | 0.015 | -0.282 | 0.011 | -19.39 | 1.62 |
| YZ Boo | 231.02917 | 36.86683 | DSCT | 0.104092 | 0.026 | 2015-03-09 | A7V | 7339.1 | 7.96 | 4.053 | 0.009 | -0.3 | 0.008 | -22.48 | 1.49 |
| BS Cnc | 129.78792 | 19.59239 | DSCTC | 0.051 | 0.047 | 2015-03-08 | A7V | 7458.88 | 2.27 | 3.928 | 0.001 | 0.064 | 0.002 | 27.42 | 0.5 |
| BS Cnc | 129.78792 | 19.59239 | DSCTC | 0.051 | 0.047 | 2015-10-30 | A7V | 7486.35 | 10.19 | 3.877 | 0.013 | 0.072 | 0.01 | 4.73 | 1.4 |
| BS Cnc | 129.78792 | 19.59239 | DSCTC | 0.051 | 0.047 | 2016-01-27 | F0 | 7495.34 | 15.16 | 3.89 | 0.02 | 0.073 | 0.014 | 35.75 | 1.71 |
| BS Cnc | 129.78792 | 19.59239 | DSCTC | 0.051 | 0.047 | 2016-02-24 | A5V | 7465.01 | 2.68 | 3.915 | 0.002 | 0.037 | 0.002 | 27.71 | 0.59 |
| BV Cnc | 130.13733 | 19.19433 | DSCTC | 0.21 | 0.023 | 2015-10-30 | A7V | 7313.94 | 3.16 | 3.963 | 0.002 | 0.229 | 0.003 | 30.32 | 0.69 |
| BV Cnc | 130.13733 | 19.19433 | DSCTC | 0.21 | 0.023 | 2016-02-24 | F0 | 7335.62 | 2.07 | 3.925 | 0.001 | 0.238 | 0.002 | 31.17 | 0.45 |
| BW Cnc | 130.21867 | 20.26653 | DSCTC | 0.072 | 0.063 | 2015-03-08 | A7V | 7419.46 | 7.05 | 3.917 | 0.004 | 0.119 | 0.006 | 30.54 | 1.57 |
| BW Cnc | 130.21867 | 20.26653 | DSCTC | 0.072 | 0.063 | 2015-10-30 | F0 | 7401.68 | 2.07 | 3.883 | 0.001 | 0.129 | 0.002 | 33.16 | 0.45 |
| BW Cnc | 130.21867 | 20.26653 | DSCTC | 0.072 | 0.063 | 2016-01-27 | F0 | 7491.59 | 2.56 | 3.898 | 0.002 | 0.147 | 0.002 | 23.8 | 0.62 |
| BW Cnc | 130.21867 | 20.26653 | DSCTC | 0.072 | 0.063 | 2016-02-24 | A6IV | 7407.39 | 2.14 | 3.914 | 0.001 | 0.122 | 0.002 | 31.22 | 0.47 |
| GP Cnc | 129.5405 | 7.22583 | DSCTC | | 0.225 | 2015-02-06 | F0 | 7321.92 | 8.92 | 4.121 | 0.011 | -0.389 | 0.008 | -11.45 | 1.2 |
| UX LMi | 161.42579 | 27.96506 | DSCT | 0.15064 | 0.082 | 2011-12-26 | F0 | 6822.54 | 267.41 | 3.53 | 0.382 | 0.414 | 0.249 | -13.89 | 20.61 |
| UX LMi | 161.42579 | 27.96506 | DSCT | 0.15064 | 0.082 | 2011-12-15 | F0 | 7050.22 | 9.78 | 3.671 | 0.006 | 0.44 | 0.008 | -8.25 | 2.17 |
| WW LMi | 163.67571 | 25.49072 | DSCTC | 0.12691 | 0.083 | 2012-01-04 | F0 | 7195.51 | 12.84 | 3.789 | 0.016 | 0.297 | 0.012 | 14.88 | 1.85 |
| WW LMi | 163.67571 | 25.49072 | DSCTC | 0.12691 | 0.083 | 2012-03-11 | F0 | 7242.71 | 18.85 | 3.738 | 0.026 | 0.279 | 0.018 | 15.34 | 2.06 |
| V0501 Per | 63.96912 | 51.21828 | DSCT | | 0.529 | 2012-02-08 | F0 | 7144.9 | 132.82 | 4.258 | 0.189 | -0.139 | 0.124 | -13.03 | 10.46 |
| UV Tri | 23.00046 | 30.36569 | DSCTC | | 0.184 | 2013-10-04 | F0 | 7254.66 | 13.57 | 3.891 | 0.018 | 0.142 | 0.013 | 25.23 | 1.71 |
| V0460 And | 38.55942 | 42.241 | DSCT | 0.074981 | 0.071 | 2014-11-04 | A6IV | 8116.29 | 32.49 | 4.164 | 0.045 | -0.247 | 0.031 | -77.13 | 3.15 |
| NSV 1273 | 56.39346 | 24.46328 | DSCT: | | 0.363 | 2016-09-30 | A6IV | 7293.98 | 2.65 | 4.076 | 0.002 | -0.1 | 0.002 | 2.94 | 0.58 |
| NSV 1273 | 56.39346 | 24.46328 | DSCT: | | 0.363 | 2016-11-10 | A6IV | 7316.69 | 6.29 | 4.107 | 0.007 | -0.078 | 0.002 | 1.57 | 1.16 |
| V1116 Her | 247.56833 | 16.91833 | DSCT | 0.094683 | 0.166 | 2013-04-20 | A7V | 7748.59 | 3.9 | 4.119 | 0.002 | -0.408 | 0.003 | -71.86 | 0.85 |
| NSV 12196 | 293.82446 | 46.419 | DSCT | 0.052768 | 0.982 | 2012-06-04 | A7V | 7429.25 | 2.77 | 3.913 | 0.002 | 0.091 | 0.002 | -30.01 | 0.65 |
| NSV 19942 | 205.9122 | 21.0957 | DSCT | 0.16352 | 0.13 | 2015-01-23 | F0 | 7048.45 | 26.42 | 3.748 | 0.035 | 0.436 | 0.025 | -1.57 | 3.06 |
| ASAS J012242+0854.1 | 20.67687 | 8.90192 | DSCT | 0.067416 | 0.061 | 2015-12-11 | A7V | 7375.75 | 22.23 | 4.183 | 0.028 | -0.446 | 0.021 | -42.84 | 3.05 |
| ASAS J024816+2213.4 | 42.06658 | 22.22214 | DSCT | 0.080315 | 0.064 | 2015-01-18 | F0 | 7291.11 | 2.45 | 3.886 | 0.002 | 0.011 | 0.002 | 17.4 | 0.54 |
| ASAS J030012+0731.1 | 45.05079 | 7.51789 | DSCT | 0.067219 | 0.013 | 2012-11-01 | A5V | 7439.49 | 6.23 | 4.136 | 0.006 | -0.44 | 0.006 | -31.26 | 1.39 |
| ASAS J041335+1436.5 | 63.39458 | 14.60917 | DSCT | 0.184713 | 0.912 | 2014-10-15 | F0 | 7010.45 | 8.25 | 3.662 | 0.007 | 0.219 | 0.008 | -35.77 | 1.93 |
| ASAS J053536+1156.6 | 83.89804 | 11.944 | DSCT | 0.128574 | 0.072 | 2016-02-20 | F0 | 6940.76 | 5.02 | 3.69 | 0.004 | 0.15 | 0.005 | -45.46 | 1.2 |
| ASAS J054242+2220.0 | 85.67637 | 22.33244 | DSCT | 0.092596 | 0.108 | 2013-12-20 | F0 | 7215.78 | 9.44 | 3.941 | 0.011 | -0.041 | 0.009 | 1.04 | 1.57 |
| ASAS J060757-0207.7 | 91.98754 | -2.12881 | DSCT | 0.161646 | 0.064 | 2013-02-22 | F0 | 6777.89 | 212.69 | 3.831 | 0.305 | 0.33 | 0.198 | 24.53 | 15.7 |
| ASAS J061149+1248.0 | 92.95433 | 12.79972 | DSCT | 0.192694 | 0.198 | 2014-01-03 | F0 | 7040.28 | 6.7 | 3.67 | 0.004 | 0.384 | 0.006 | 39.49 | 1.47 |
| ASAS J063309+1810.8 | 98.28758 | 18.17931 | DSCT | 0.071253 | 0.108 | 2014-02-17 | F0 | 7280.16 | 90.74 | 3.892 | 0.129 | -0.199 | 0.085 | 12.45 | 7.47 |
| ASAS J063515-0115.3 | 98.81054 | -1.25547 | DSCT—ESD—ED | 0.14244 | 0.095 | 2014-11-19 | F0 | 7165.1 | 52.56 | 3.93 | 0.074 | 0.037 | 0.049 | -4.33 | 4.52 |
| ASAS J064317+0942.8 | 100.82 | 9.71306 | DSCT | 0.116271 | 0.194 | 2012-02-02 | A6IV | 7224.68 | 11.91 | 3.903 | 0.015 | -0.161 | 0.011 | -11.74 | 1.77 |
| ASAS J064624+1107.1 | 101.60088 | 11.11719 | DSCT—RRC—EC | 0.219591 | 0.007 | 2012-02-10 | F0 | 6919.39 | 117.33 | 3.581 | 0.167 | 0.434 | 0.11 | 18.59 | 9.39 |
| ASAS J070621+2024.7 | 106.58917 | 20.41231 | DSCT—ED | 0.040483 | 0.049 | 2016-03-27 | F0 | 6841.46 | 21.45 | 3.998 | 0.029 | -0.006 | 0.02 | 28.38 | 2.35 |
| ASAS J070907+2656.7 | 107.27883 | 26.94475 | DSCT—ESD | 0.043322 | 0.161 | 2013-03-13 | F6 | 6438.88 | 28.08 | 4.18 | 0.039 | 0.079 | 0.026 | 21.71 | 2.71 |
| ASAS J073954-0206.2 | 114.97483 | -2.10319 | DSCT | 0.101629 | 0.029 | 2014-12-04 | F0 | 7244.39 | 5.18 | 3.857 | 0.005 | -0.023 | 0.005 | -4.11 | 1.18 |
| ASAS J074248+0001.8 | 115.7015 | 0.03036 | DSCT—BCEP | 0.109313 | 0.047 | 2014-12-04 | A6IV | 7268.07 | 3.27 | 4.046 | 0.002 | -0.183 | 0.003 | -18.55 | 0.72 |
| ASAS J075941-0353.1 | 119.91925 | -3.88594 | DSCT—BCEP—EC—ESD—ED | 0.180982 | 0.104 | 2013-11-20 | F0 | 7041.45 | 2.6 | 3.766 | 0.002 | 0.166 | 0.002 | -3.03 | 0.57 |
| ASAS J075941-0353.1 | 119.91925 | -3.88594 | DSCT—BCEP—EC—ESD—ED | 0.180982 | 0.104 | 2013-11-20 | F0 | 7045.52 | 3.07 | 3.701 | 0.002 | 0.178 | 0.003 | -5.63 | 0.75 |
| ASAS J075941-0353.1 | 119.91925 | -3.88594 | DSCT—BCEP—EC—ESD—ED | 0.180982 | 0.104 | 2013-11-20 | F0 | 7049.03 | 3.58 | 3.757 | 0.002 | 0.182 | 0.003 | -5.36 | 0.78 |
| ASAS J075941-0353.1 | 119.91925 | -3.88594 | DSCT—BCEP—EC—ESD—ED | 0.180982 | 0.104 | 2012-12-22 | F0 | 7078.3 | 154.31 | 3.746 | 0.22 | 0.136 | 0.144 | -16.15 | 12.26 |
| ASAS J075941-0353.1 | 119.91925 | -3.88594 | DSCT—BCEP—EC—ESD—ED | 0.180982 | 0.104 | 2012-12-22 | F0 | 7099.22 | 10.22 | 3.773 | 0.013 | 0.187 | 0.01 | -3.46 | 1.45 |
| ASAS J075941-0353.1 | 119.91925 | -3.88594 | DSCT—BCEP—EC—ESD—ED | 0.180982 | 0.104 | 2012-12-22 | F0 | 7122.39 | 22.8 | 3.771 | 0.031 | 0.187 | 0.022 | -11.11 | 2.47 |
| ASAS J081425+0434.1 | 123.60479 | 4.56806 | DSCT—EC—ESD | 0.126226 | 0.275 | 2014-01-12 | F0 | 7078.43 | 4.65 | 3.809 | 0.003 | 0.074 | 0.004 | -28.47 | 1.04 |
| ASAS J081425+0434.1 | 123.60479 | 4.56806 | DSCT—EC—ESD | 0.126226 | 0.275 | 2014-01-12 | F0 | 7103.23 | 11.43 | 3.841 | 0.014 | 0.062 | 0.011 | -27.52 | 1.71 |

Table 4: Spectral types of δ Scuti stars derived by LAMOST (the first 50 observations).

| Name | R.A. (deg) | Dec. (deg) | Type | Period (days) | Distance | Date | Sp. |
|---------------------|------------|------------|---------------------|---------------|----------|------------|-------|
| BV Cnc | 130.1373 | 19.19433 | DSCTC | 0.21 | 0.023 | 2016-01-27 | A7V |
| QS Gem | 101.6195 | 20.84358 | DSCT | 0.134613 | 0.063 | 2016-03-10 | A1V |
| WW LMi | 163.6757 | 25.49072 | DSCTC | 0.12691 | 0.083 | 2012-03-10 | A8III |
| SZ Lyn | 122.399 | 44.47156 | DSCT | 0.12053492 | 0.029 | 2014-11-10 | A6IV |
| V0783 Mon | 103.0424 | 2.71408 | DSCT | | 0.037 | 2015-10-11 | A2IV |
| V1162 Ori | 83.00829 | -7.25683 | DSCT | 0.078684 | 0.065 | 2013-11-20 | A7V |
| V0459 Per | 50.49425 | 49.21486 | DSCTC | 0.037 | 0.025 | 2014-11-09 | A7V |
| UV Tri | 23.00046 | 30.36569 | DSCTC | | 0.149 | 2014-12-01 | G5 |
| NSV 25890 | 336.0433 | -2.06194 | DSCTC | | 0.742 | 2012-10-04 | A7V |
| ASAS J010803+0201.4 | 17.01146 | 2.02386 | DSCT | 0.207325 | 0.051 | 2012-09-28 | F9 |
| ASAS J020653+0815.6 | 31.71892 | 8.26008 | DSCT—EC—ESD | 0.177637 | 0.084 | 2012-09-29 | G3 |
| ASAS J020653+0815.6 | 31.71892 | 8.26008 | DSCT—EC—ESD | 0.177637 | 0.084 | 2012-10-04 | G4 |
| ASAS J033133+0501.8 | 52.88833 | 5.02919 | DSCT | 0.207452 | 0.082 | 2014-12-02 | F0 |
| ASAS J041353+0305.8 | 63.47246 | 3.09778 | DSCT | 0.053083 | 0.066 | 2015-11-29 | A7V |
| ASAS J062805+0453.8 | 97.02042 | 4.89778 | DSCT—EC—ESD | 0.076292 | 0.805 | 2016-03-21 | A7V |
| ASAS J062805+0453.8 | 97.02042 | 4.89778 | DSCT—EC—ESD | 0.076292 | 0.781 | 2013-01-03 | A7V |
| ASAS J071520+0543.6 | 108.8311 | 5.72636 | DSCT—EC—ESD | 0.142889 | 0.089 | 2015-11-03 | A7IV |
| ASAS J071838+2819.9 | 109.6582 | 28.33111 | DSCT | 0.11179 | 0.126 | 2013-03-13 | F6 |
| ASAS J073955+1313.7 | 114.9773 | 13.22769 | DSCT | 0.160825 | 0.046 | 2015-12-29 | F0 |
| ASAS J075605+2334.0 | 119.0206 | 23.566 | DSCT—BCEP—EC—ESD | 0.147703 | 0.162 | 2012-12-04 | A2IV |
| ASAS J075605+2334.0 | 119.0206 | 23.566 | DSCT—BCEP—EC—ESD | 0.147703 | 0.162 | 2013-11-29 | A3IV |
| ASAS J075941-0353.1 | 119.9193 | -3.88594 | DSCT—BCEP—EC—ESD—ED | 0.180982 | 0.104 | 2012-12-24 | F0 |
| ASAS J075941-0353.1 | 119.9193 | -3.88594 | DSCT—BCEP—EC—ESD—ED | 0.180982 | 0.104 | 2012-12-24 | F0 |
| ASAS J080015+2821.0 | 120.0647 | 28.34953 | DSCT—BCEP | 0.11174 | 0.101 | 2012-12-31 | A3IV |
| ASAS J080015+2821.0 | 120.0647 | 28.34953 | DSCT—BCEP | 0.11174 | 0.101 | 2012-12-31 | A3IV |
| ASAS J084602+1301.4 | 131.5059 | 13.02433 | DSCT—BCEP | 0.121261 | 0.087 | 2016-02-06 | A7V |
| ASAS J090228+2604.9 | 135.6155 | 26.08139 | DSCT | 0.100453 | 0.119 | 2012-03-07 | A7V |
| ASAS J091211+1347.2 | 138.0447 | 13.78547 | DSCT—EC—ESD | 0.183637 | 0.110 | 2014-03-24 | A2V |
| ASAS J095515+0239.0 | 148.8142 | 2.65036 | DSCT—EC | 0.170812 | 0.018 | 2012-11-26 | F2 |
| ASAS J095515+0239.0 | 148.8142 | 2.65036 | DSCT—EC | 0.170812 | 0.018 | 2012-12-24 | F8 |
| ASAS J100201+1859.4 | 150.5057 | 18.99108 | DSCT | 0.116286 | 0.082 | 2013-01-09 | F5 |
| ASAS J105152-0142.5 | 162.9688 | -1.70822 | DSCT—RRC—EC—ESD | 0.218867 | 0.094 | 2014-01-09 | F0 |
| ASAS J111452+0050.6 | 168.7149 | 0.84408 | DSCT | 0.168321 | 0.016 | 2012-12-21 | G3 |
| ASAS J120957+1103.5 | 182.4885 | 11.05872 | DSCT | 0.161364 | 0.018 | 2013-02-05 | G4 |
| ASAS J121536-0350.4 | 183.8988 | -3.8395 | DSCT—EC—ESD | 0.189077 | 0.272 | 2014-01-02 | A7III |
| ASAS J130538-0146.4 | 196.4081 | -1.77206 | DSCT—EC | 0.130645 | 0.087 | 2014-03-10 | K5 |
| ASAS J141600-0042.6 | 214.0007 | -0.70986 | DSCT | 0.157321 | 0.059 | 2013-03-05 | G5 |
| ASAS J145224+0318.5 | 223.0989 | 3.30878 | DSCT | 0.112351 | 0.410 | 2014-01-29 | A5V |
| ASAS J145224+0318.5 | 223.0989 | 3.30878 | DSCT | 0.112351 | 0.410 | 2014-03-24 | A6IV |
| ASAS J152257+1054.4 | 230.7351 | 10.90667 | DSCT | 0.054955 | 0.106 | 2014-06-03 | A6IV |
| ASAS J152940+1359.0 | 232.4171 | 13.98225 | DSCT | 0.0759 | 0.170 | 2016-04-24 | A7V |
| ASAS J152940+1359.0 | 232.4171 | 13.98225 | DSCT | 0.0759 | 0.031 | 2013-03-02 | A7V |
| ASAS J152940+1359.0 | 232.4171 | 13.98225 | DSCT | 0.0759 | 0.031 | 2013-03-02 | A6IV |
| ASAS J154239-0145.6 | 235.6614 | -1.75897 | DSCT—BCEP—ESD—ED | 0.079036 | 0.036 | 2016-05-18 | A7IV |
| ASAS J155522+1844.1 | 238.8404 | 18.73578 | DSCT—EC | 0.066599 | 0.053 | 2015-05-23 | A6IV |
| ASAS J175048+0002.8 | 267.7 | 0.04661 | DSCT—EC | 0.149961 | 0.041 | 2016-05-17 | A5V |
| ASAS J184120+2327.3 | 280.3332 | 23.45672 | DSCT—RRC—EC—ESD | 0.225343 | 0.204 | 2014-04-19 | O |
| ASAS J214518-0526.0 | 326.3239 | -5.43294 | DSCT—EC | 0.177296 | 0.057 | 2012-09-30 | F9 |
| ASAS J214604+0327.6 | 326.5168 | 3.459 | DSCT—EC | 0.17361 | 0.014 | 2012-10-02 | G1 |
| ASAS J231947+1244.0 | 349.9457 | 12.73308 | DSCT—RRC—EC | 0.21286 | 0.125 | 2012-10-29 | F5 |

Table 5: Ten δ Scuti variable stars with the highest metallicities.

| Name | $\alpha(2000)$ | $\delta(2000)$ | Period (days) | Sp. | T (K) | $\log g$ | [Fe/H] | V_r (km s $^{-1}$) |
|---------------------|----------------|----------------|---------------|-----|---------|----------|--------|-----------------------|
| KIC 10014548 | 293.05929 | 46.90581 | 0.65445 | F0 | 7210.29 | 3.815 | 0.561 | -68.64 |
| KID 07900367 | 294.93729 | 43.69592 | 0.075489 | F0 | 7197.27 | 3.805 | 0.513 | -24.23 |
| BD+24 95 | 10.26 | 25.26081 | 0.11992 | F0 | 7089.90 | 3.750 | 0.490 | -18.60 |
| KIC 8103917 | 294.03021 | 43.91889 | 0.056348 | F0 | 7308.51 | 3.816 | 0.490 | -29.05 |
| KIC 9874181 | 282.86071 | 46.78 | 0.049222 | F0 | 7440.01 | 3.814 | 0.490 | -28.81 |
| KIC 5722346 | 296.3865 | 40.94497 | 0.0883 | F0 | 7161.11 | 3.800 | 0.460 | -19.88 |
| KIC 4936524 | 295.20129 | 40.04136 | 0.035665 | F0 | 7389.75 | 3.835 | 0.457 | -6.65 |
| KIC 5038228 | 298.18271 | 40.18222 | 1.10619 | F0 | 7183.76 | 3.731 | 0.437 | -69.34 |
| NSV 19942 | 205.9122 | 21.0957 | 0.16352 | F0 | 7048.45 | 3.748 | 0.436 | -1.57 |
| ASAS J064624+1107.1 | 101.60088 | 11.11719 | 0.219591 | F0 | 6919.39 | 3.581 | 0.434 | 18.59 |

Table 6: 36 δ Scuti pulsating stars with the difference of radial velocity larger than 15 km s $^{-1}$.

| Name | Period (days) | Dates | Times | T (K) | $\log g$ | [Fe/H] | V_{Low} | V_{High} | ΔV |
|----------------------------|---------------|-----------------------|-------|---------|----------|--------|-----------|------------|------------|
| KIC 5722346 | 0.0883 | 2013-10-05–2015-10-08 | 3 | 7161.11 | 3.800 | 0.460 | -53.48 | 11.26 | 64.74 |
| ASAS J081813-0049.8 | 0.139603 | 2013-11-25–2015-02-05 | 2 | 7117.51 | 3.803 | 0.214 | -47.11 | 11.06 | 58.17 |
| KIC 10014548 | 0.65445 | 2012-06-04–2015-10-02 | 9 | 7210.29 | 3.815 | 0.561 | -101.68 | -50.10 | 51.58 |
| ASAS J085536+0215.5 | 0.207902 | 2012-02-10–2016-04-03 | 3 | 5955.84 | 4.227 | -0.396 | -24.82 | 18.37 | 43.19 |
| ASAS J154613-0026.1 | 0.068991 | 2012-05-16–2016-05-18 | 3 | 7427.65 | 4.119 | -0.358 | -9.86 | 26.90 | 36.76 |
| KIC 7350486 | 0.75188 | 2013-09-26–2016-05-18 | 3 | 7127.45 | 3.894 | 0.097 | -59.48 | -24.93 | 34.55 |
| KIC 4252757 | 0.046555 | 2012-06-15–2014-06-02 | 2 | 7503.30 | 3.954 | -0.046 | -67.98 | -34.19 | 33.79 |
| KIC 3634384 | 0.085852 | 2012-06-15–2014-06-02 | 3 | 7361.62 | 3.869 | 0.096 | -5.05 | 26.75 | 31.8 |
| BS Cnc | 0.051 | 2015-03-08–2016-02-24 | 4 | 7476.40 | 3.902 | 0.062 | 4.73 | 35.75 | 31.02 |
| KIC 5476864 | 0.59988 | 2013-10-05–2014-05-22 | 2 | 7064.31 | 4.115 | 0.093 | -38.08 | -8.62 | 29.46 |
| KIC 3942911 | 0.03391 | 2012-06-15–2015-10-12 | 6 | 7436.53 | 3.956 | 0.047 | -39.34 | -10.57 | 28.77 |
| NSVS 3820963 | 0.16784703 | 2014-11-04–2015-12-28 | 2 | 5701.43 | 4.271 | -0.123 | -97.83 | -70.77 | 27.06 |
| BD+24 95 | 0.11992 | 2012-09-29–2013-12-19 | 4 | 7089.90 | 3.750 | 0.490 | -32.97 | -6.77 | 26.20 |
| KIC 9391395 | 0.51308 | 2014-05-02–2015-09-25 | 4 | 7246.77 | 4.046 | -0.198 | -29.52 | -3.51 | 26.01 |
| KIC 8429756 | 0.036041 | 2013-05-19–2015-10-11 | 2 | 6786.47 | 3.935 | -0.085 | -31.27 | -5.79 | 25.48 |
| LINEAR 9272851 | 0.080104 | 2016-01-13–2016-02-06 | 2 | 7138.87 | 4.250 | -0.903 | 248.64 | 272.74 | 24.10 |
| ASAS J075428+1407.8 | 0.189175 | 2013-02-15–2013-12-14 | 3 | 6058.86 | 4.288 | -0.406 | 29.01 | 53.03 | 24.02 |
| V0367 Cam | 0.121596 | 2012-01-13–2016-01-19 | 4 | 7307.84 | 3.857 | 0.188 | -15.90 | 7.36 | 23.26 |
| KIC 11193046 | 0.78431 | 2013-05-22–2015-10-02 | 2 | 8006.16 | 3.862 | -0.085 | -24.84 | -2.11 | 22.73 |
| KIC 7106205 | 0.074655 | 2013-05-19–2015-10-11 | 7 | 7165.09 | 3.838 | 0.117 | -29.48 | -9.87 | 19.61 |
| ASAS J083952+0052.4 | 0.133043 | 2013-03-24–2013-03-24 | 2 | 4626.97 | 4.364 | 0.030 | 50.87 | 70.01 | 19.14 |
| ASAS J064626+2629.8 | 0.205972 | 2012-03-11–2016-01-18 | 4 | 6609.64 | 4.163 | -0.249 | -0.46 | 18.51 | 18.97 |
| KIC 9450940 | 0.033337 | 2014-05-29–2015-10-06 | 3 | 7922.96 | 4.056 | -0.19 | -60.70 | -41.88 | 18.82 |
| BD+38 2361 | 0.049839 | 2014-01-12–2016-01-28 | 2 | 7467.20 | 3.953 | -0.095 | -34.15 | -15.68 | 18.47 |
| KID 6593488 | 0.10101 | 2015-09-25–2016-05-18 | 3 | 7027.68 | 3.961 | -0.088 | -42.48 | -24.22 | 18.26 |
| KIC 8460993 | 0.05535 | 2013-09-25–2015-10-03 | 2 | 7179.78 | 3.862 | 0.245 | -67.62 | -49.68 | 17.94 |
| ASAS J190751+4629.2 | 0.079561 | 2013-10-04–2015-05-30 | 4 | 7178.47 | 3.912 | 0.185 | -71.42 | -54.07 | 17.35 |
| NSVS 9420734 | 0.19695349 | 2014-09-17–2016-02-10 | 3 | 6018.85 | 3.982 | 0.030 | -19.83 | -2.73 | 17.10 |
| GSC 01946-00035 | 0.06708077 | 2013-12-01–2014-12-02 | 4 | 7264.50 | 3.997 | -0.028 | 58.80 | 75.89 | 17.09 |
| ASAS J163007+0125.2 | 0.160533 | 2013-03-24–2013-03-24 | 2 | 5550.52 | 4.213 | -0.215 | -33.01 | -16.34 | 16.67 |
| KIC 9052363 | 0.023829 | 2013-09-25–2015-10-03 | 3 | 7841.68 | 4.076 | -0.151 | -32.47 | -16.25 | 16.22 |
| HAT 199-00623 | 0.29481 | 2012-06-17–2015-10-18 | 2 | 6982.10 | 3.537 | 0.427 | -75.27 | -59.09 | 16.18 |
| 1SWASP J032748.43+343810.3 | 0.11771 | 2013-09-14–2014-11-01 | 2 | 7166.28 | 3.950 | -0.256 | -30.33 | -14.52 | 15.81 |
| KIC 7977996 | 0.090662 | 2013-10-05–2015-10-08 | 2 | 7317.98 | 4.133 | -0.108 | 1.58 | 17.07 | 15.49 |
| NSVS 9431318 | 0.17746757 | 2014-10-05–2014-11-01 | 2 | 6101.04 | 4.072 | -0.557 | 48.61 | 64.07 | 15.46 |
| ASAS J093944+0010.3 | 0.196522 | 2012-02-16–2015-01-03 | 2 | 6191.79 | 4.190 | -0.227 | 28.69 | 43.88 | 15.19 |

Table 7: 28 δ Scuti variable stars with radial velocities higher than 70 km s^{-1} .

| Name | Period (days) | Sp. | T (K) | $\log g$ | [Fe/H] | V_r (km s^{-1}) |
|----------------------|---------------|------|---------|----------|--------|------------------------------|
| LINEAR 9272851 | 0.080104 | A7V | 7060.11 | 4.231 | -0.937 | 272.74 |
| KID 8004558 | 0.042706 | A5V | 7454.12 | 4.286 | -0.891 | -262.45 |
| LINEAR 9272851 | 0.080104 | A7V | 7217.63 | 4.270 | -0.869 | 248.64 |
| LINEAR 23008936 | 0.060405 | A5V | 7319.02 | 4.237 | -0.736 | 199.62 |
| LINEAR 565638 | 0.086365 | A7IV | 6751.99 | 4.228 | -0.740 | -176.72 |
| ASAS J175302+0405.7 | 0.15565 | K1 | 5240.85 | 4.280 | 0.295 | -130.81 |
| LINEAR 19119847 | 0.080278 | A7V | 7327.85 | 4.159 | -0.271 | -121.87 |
| KIC 10014548 | 0.65445 | F0 | 7232.51 | 3.738 | 0.581 | -101.68 |
| Renson 31680 | 0.46666 | A7V | 7568.18 | 4.120 | -0.357 | -99.06 |
| NSVS 3820963 | 0.16784703 | G4 | 5742.78 | 4.286 | -0.115 | -97.83 |
| KIC 10014548 | 0.65445 | F0 | 7233.08 | 3.839 | 0.574 | -95.89 |
| Renson 31680 | 0.46666 | A7V | 7541.54 | 4.095 | -0.368 | -95.48 |
| Renson 31680 | 0.46666 | A7V | 7478.40 | 4.118 | -0.357 | -93.78 |
| ASAS J053125+1103.8 | 0.144799 | F2 | 5966.68 | 4.229 | -0.330 | 88.38 |
| CR Ari | 0.18094 | A2V | 7110.43 | 3.919 | -0.788 | -86.80 |
| ASAS J022414+2741.6 | 0.155998 | G3 | 5688.79 | 4.231 | -0.058 | -84.62 |
| ASAS J152257+1054.4 | 0.054955 | A5V | 8284.55 | 4.070 | -0.311 | -83.29 |
| ASAS J053125+1103.8 | 0.144799 | F8 | 5857.76 | 4.081 | -0.428 | 81.63 |
| ASAS J170044-0241.3 | 0.160861 | G2 | 5754.02 | 3.990 | -0.258 | -79.65 |
| ASAS J151411+2043.1 | 0.212255 | G4 | 5657.75 | 4.094 | 0.039 | -79.09 |
| ASAS J135248+1150.2 | 0.186274 | F5 | 6342.55 | 4.230 | -0.467 | -78.67 |
| KIC 10014548 | 0.65445 | F0 | 7228.09 | 3.816 | 0.586 | -77.28 |
| V0460 And | 0.0749808 | A6IV | 8116.29 | 4.164 | -0.247 | -77.13 |
| ASAS J084602+1301.4 | 0.121261 | F0 | 7342.00 | 3.926 | 0.120 | 76.71 |
| GSC 01946-00035 | 0.06708077 | F0 | 7205.42 | 3.976 | 0.006 | 75.89 |
| HAT 199-00623 | 0.29481 | F0 | 7029.38 | 3.588 | 0.433 | -75.27 |
| CSS_J085942.7+190007 | 0.1809983 | F2 | 6164.71 | 4.300 | -0.489 | -74.89 |
| KIC 5038228 | 1.10619 | F0 | 7252.92 | 3.616 | 0.447 | -73.50 |
| ASAS J084602+1301.4 | 0.121261 | F0 | 7570.18 | 3.919 | 0.078 | 72.12 |
| V1116 Her | 0.094683 | A7V | 7748.59 | 4.119 | -0.408 | -71.86 |
| VSX J175138.3+373909 | 0.04038 | A7V | 7565.68 | 3.861 | 0.106 | -71.81 |
| ASAS J190751+4629.2 | 0.079561 | F0 | 7185.31 | 3.932 | 0.168 | -71.42 |
| Galati V3 | 0.098 | F0 | 7185.47 | 3.959 | 0.062 | -71.04 |
| ASAS J155047+0505.4 | 0.15218 | G3 | 5728.19 | 4.186 | -0.176 | -70.94 |
| NSVS 3820963 | 0.16784703 | G3 | 5660.09 | 4.256 | -0.132 | -70.77 |
| ASAS J083952+0052.4 | 0.133043 | K5 | 4551.25 | 4.362 | 0.035 | 70.01 |

Table 8: LAMOST observations of δ Scuti variable stars without periods listed in VSX.

| Name | $\alpha(2000)$ | $\delta(2000)$ | Dates | Sp. | T (K) | $\log g$ | [Fe/H] | V_r (km s ⁻¹) |
|--------------------|----------------|----------------|------------|------|---------|----------|--------|-----------------------------|
| GP Cnc | 129.5405 | 7.22583 | 2015-02-06 | F0 | 7321.92 | 4.121 | -0.389 | -11.45 |
| V0501 Per | 63.96912 | 51.21828 | 2012-02-08 | F0 | 7144.90 | 4.258 | -0.139 | -13.03 |
| UV Tri | 23.00046 | 30.36569 | 2013-10-04 | F0 | 7254.66 | 3.891 | 0.142 | 25.23 |
| NSV 1273 | 56.39346 | 24.46328 | 2016-09-30 | A6IV | 7293.98 | 4.076 | -0.100 | 2.94 |
| NSV 1273 | 56.39346 | 24.46328 | 2016-11-10 | A6IV | 7316.69 | 4.107 | -0.078 | 1.57 |
| [EHV2002] 1-5-0832 | 91.85333 | 45.9975 | 2013-12-15 | F0 | 6980.23 | 4.110 | -0.385 | -41.01 |
| HD 12899 | 31.67329 | 14.58378 | 2012-09-30 | F0 | 7165.54 | 3.849 | 0.059 | -15.08 |
| HD 89503 | 154.9601 | 7.61394 | 2015-04-24 | A7V | 7445.30 | 3.870 | -0.025 | -4.61 |
| HD 89503 | 154.9601 | 7.61394 | 2016-01-22 | F0 | 7542.13 | 3.790 | -0.076 | 0.50 |
| BD+19 572 | 55.00588 | 19.81067 | 2016-01-29 | K1 | 5065.33 | 2.844 | 0.049 | 16.53 |
| BD+16 1693 | 125.09 | 15.86461 | 2016-03-13 | F0 | 7125.94 | 3.816 | 0.102 | 12.43 |
| HD 221012 | 352.119 | 18.69408 | 2014-11-05 | A7V | 7611.00 | 4.005 | 0.003 | 0.02 |